Numerical investigation of Newhouse sinks of Hénon map

Takayuki Yamaguchi

Department of Mathematics, Hokkaido University, Kita 10, Nishi 8, Kita-Ku, Sapporo, Hokkaido, 060-0810, Japan
E-mail address: yt@math.sci.hokudai.ac.jp

Contents

Introduction

In this paper we investigate numerically Newhouse sinks of Hénon map. For nearly classical parameter values of Hénon map, we search numerically for a sequence of Newhouse sinks and investigate their basins and average rambling time.

Firstly, we obtain the first few Newhouse sinks by using an algorithm based on the proof of existences of Newhouse sinks and investigate the basin of attraction of the sink. In the case that we observed, when the sink exists, most orbits converge to it, and the orbit that seems to be Hénon attractor is not an attractor but just a long chaotic transient. The appearances of Newhouse sinks in our cases cause the changes from Hénon attractor to a long chaotic transient.

Secondly, we show how to find successively the Newhouse sinks of higher period. In general, simple iterations of some initial points converge to an attractor. However, it is difficult for simple iterations of some initial points to find Newhouse sinks because the parameter ranges in which these sinks exist are too short. It is known that properties of Newhouse sinks satisfy power laws. We estimate the parameter values and coordinates of the succeeding Newhouse sinks from the power laws and search in a neighborhood of the estimation values by simple iterations. From our estimation, we obtained numerically a sequence of sinks of period from 8 to 60. We also show numerical data of power laws of the sequence of the sinks.

Thirdly, we verify our obtained sinks by applying Brouwer fixed point theorem with interval arithmetic. Fourthly, we discuss the rambling time of the chaotic transients of these sinks.

The sequence of sinks are constructed to prove coexistence of infinitely many sinks. Newhouse showed coexistence of infinitely many sinks when a one-parameter family of two dimensional dissipative diffeomorphism creates a homoclinic tangency nondegenerately [**New74, New79**]. For a homoclinic tangency, there exists a horseshoe in a neighborhood of the coordinate of the tangency and in a neighborhood of the parameter that the tangency occurs. When we perturb the parameter of the horseshoe, a periodic point in the horseshoe becomes stable. Such sinks at different parameters compose a sequence converging to the homoclinic tangency, which is our object in this paper. In addition, when we fix a homoclinic tangency, because of abundance of diffeomorphisms having a different homoclinic tangency in a neighborhood of the parameter of the fixed homoclinic tangency, infinitely many sinks coexist at a parameter.

The convergence of the aforementioned sequence to the homoclinic tangency means the following. If a one parameter family $\{F_t\}$ of two-dimensional dissipative diffeomorphisms has a homoclinic tangency q_0 at a parameter t_0, there is a sequence of parameters $\{t_j\}$ accumulating to t_0 such that the diffeomorphism F_{t_j} has a sink q_j of period n_j and, as j varies to infinity, the sequence of sinks $\{q_j\}$ accumulates to q_0 and the sequence n_j goes to infinity [**GS72, New74, Rob83**]. We refer to the sequence of sinks as an infinite cascade of sinks. This phenomenon gives the existence of a diffeomorphism with a sink of arbitrarily high period near a diffeomorphism having a homoclinic tangency.

Each sink in an infinite cascade of sinks is obtained as below. Perturbing a diffeomorphism with a homoclinic tangency, we can construct a horseshoe near the homoclinic tangency. To be more precise, we can take a rectangle region near the homoclinic tangency in an appropriate coordinate such that some iterations of the diffeomorphism map the rectangle back to its neighborhood and the image of the rectangle is bent and has two components of intersections with the rectangle. As the parameter varies to the homoclinic tangency the horseshoe are destroyed. Full horseshoe, that is, a situation so that the intersection of the rectangle and its image consists of two components, has two saddle periodic points. As the parameter varies slightly so as to break the full horseshoe of the dissipative diffeomorphism, one of the two saddle periodic points becomes stable. As the parameter varies further to the tangency, the subsequent horseshoes appear and destroy in turn. One sink appears in each horseshoe and these sinks in the horseshoes constitute the cascade.

We deal with only such sinks that appear in the horseshoes in a neighborhood of a homoclinic tangency. Tedeschini-Lalli and Yorke called them "simple" Newhouse sinks and investigated measure of parameters where such sinks exist [**TLY86**]. The "simple" Newhouse sinks are defined as the sinks having their orbits consisting of the following two parts: one part near the saddle fixed point mapped by almost linear map and the other part mapped by a nonlinear map. They proved that the parameters of coexistence of only infinite "simple" Newhouse sinks has zero measure. Therefore, it is not easy that we find parameter values of "simple" Newhouse sinks and we need the estimation described in the following sections.

We consider Hénon map [**Hén76**]:

$$T_{a,b}(x, y) = (1 + y - ax^2, -bx). \tag{1}$$

It is shown in [**FG92, AM06**] that the stable and unstable manifolds of the saddle fixed point $(0.631\cdots, -0.189\cdots)$ have a homoclinic tangency for the parameter a near 1.3924198079 when we fix $b = -0.3$. We deal with the same homoclinic tangency in the following sections.

An infinite cascade of sinks is governed by power laws [**CJ82, Rob83, TS94**]. We translate the power laws to estimations of parameter values and coordinates of a sequence of sinks by using calculation of stable and unstable manifolds of a fixed point. In the result, our numerical search obtained a sequence of sinks of period from 8 to 60. The sinks of period from 8 to 60 converge only in numerical experiments and and their existences of the sinks are not rigorous mathematically. We also consider the verification of the sinks. We construct numerically an inclusions in a neighborhood the sinks and apply Brouwer fixed point theorem. The verification is performed by using interval arithmetic. We proved mathematically the existences of the sinks of period from 8 to 14.

We also concerned with the basins of the sinks. In particular, for the obtained sinks, our numerical investigation shows that the basins of the sinks have intersections with the unstable manifold of the saddle fixed point. Therefore, when the sink exists, the Hénon attractor loses its stability and orbits of most initial points in phase space converge to the sink near the homoclinic tangency. Buszko and Stefański investigated transients of sinks of lower period and showed the relation of sizes of periodic windows and average rambling times [**BS06**]. We apply the same analysis of [**BS06**] to the transients of the obtained sinks. It is shown that our sinks have the same properties as the sinks of lower period in point of average rambling time.

Our numerical investigation presents an example such that Hénon attractor appeared in numerical experiments is not an attractor but just a long chaotic transient. In addition, our numerical investigation indicates that because the width of main band of the basin of the sink of high period is very narrow rounding errors

of computation hide the existences of the sinks. It is known that the parameter range of simple Newhouse sink is short and actually our numerical search for simple Newhouse sinks needs the parameter estimation. Accordingly, it is unlikely that all Hénon attractors that we observe in numerical experiments are long chaotic transients.

Acknowledgments. The author would like to thank Professor Kenji Matsumoto for all of his guidance and advice.

CHAPTER 1

Preliminaries

1. Hénon map

Hénon introduced the two-dimensional quadratic map for numerical experiments and revealed that orbits of the map show a chaotic attractor in Fig. 1 [**Hén76**]. In this paper we use the form of Hénon map (1) and the parameters in his paper correspond to $a = 1.4$ and $b = -0.3$. The map is a diffeomorphism and its inverse is

$$T_{a,b}^{-1}(x, y) = \left(-\frac{y}{b}, a\left(\frac{y}{b}\right)^2 + x - 1 \right). \tag{2}$$

If $(1 + b)^2 + 4a > 0$ then $T_{a,b}$ has two fixed points;

$$x = \frac{-(1 + b) \pm \sqrt{(1 + b)^2 + 4a}}{2a}, y = -bx. \tag{3}$$

The Jacobian matrix of $T_{a,b}$ is

$$DT_{a,b}(x, y) = \begin{pmatrix} -2ax & 1 \\ -b & 0 \end{pmatrix}. \tag{4}$$

The determinant of $DT(x, y)$ equals b and is constant.

2. Infinite cascade of sinks

In this section, we recall the construction of Newhouse sink according to [**Rob83**]. We consider a discrete dynamical system of a diffeomorphism F on R^2. Let $DF(p)$ denote the derivative of F at p. A point p is called a periodic point of period n if $F^n(p) = p$ and $F^i(p) \neq p$ for $0 < i < n$. In particular, a periodic point p of period 1 is called a fixed point. A periodic point p is called a sink if the absolute values of all eigenvalues of $DF(p)$ are less than one. A periodic point p is called a saddle periodic point if the two eigenvalues λ and μ of $DF(p)$ satisfy $|\lambda| < 1$ and $|\mu| > 1$. In addition, the periodic point p is called a dissipative periodic point if

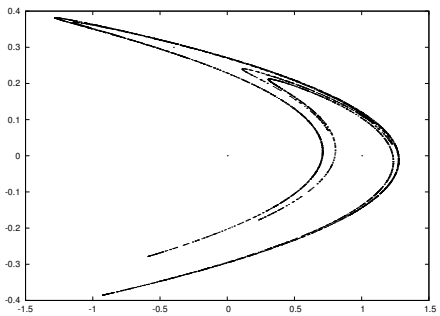

FIGURE 1. The orbits of Hénon map (1) whose initial point is (0, 0) and parameters 1.4 and −0.3.

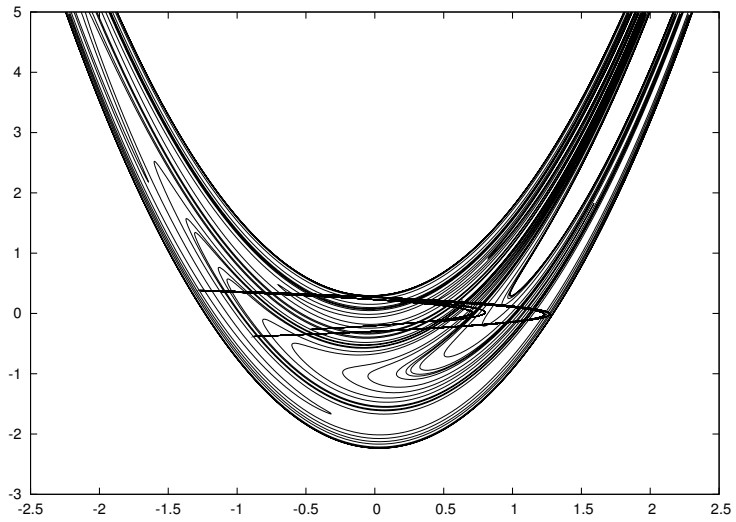

FIGURE 2. The stable and unstable manifolds of the saddle fixed point $(6.32536\cdots, 0.18976\cdots)$ of Hénon map with $a = 1.3927060035$ and $b = -0.3$ near which a homoclinic tangency occurs. The stable manifolds are the vertically long curves, which are u-shaped and reach to the top of the figure. The unstable manifolds are the horizontally long curves in the rectangle $[-1.5, 1.5]\times[-1, 1]$, which are bow-shaped and twine Hénon attractor.

$|\det DF(p)| = |\lambda\mu| < 1$. We define the stable manifold $W^s(p, F)$ and the unstable manifold $W^u(p, F)$ of a saddle fixed point p of F;

$$W^s(p, F) := \{x \in \mathbb{R}^2 \mid |f^n(p) - p| \to 0 \text{ as } n \to \infty\} \tag{5}$$

$$W^u(p, F) := \{x \in \mathbb{R}^2 \mid |f^n(p) - p| \to 0 \text{ as } n \to -\infty\}. \tag{6}$$

It is known that if F is a C^r diffeomorphism then these invariant manifolds are C^r curves and tangent to the eigendirections of $DF(p)$ at p. We call a point q a homoclinic point if q is in both $W^s(p, F)$ and $W^u(p, F)$. The homoclinic point q is called a homoclinic tangency if $W^u(q, F)$ and $W^s(q, F)$ are tangent at q. Otherwise, we call q a transverse homoclinic point.

The existence of an infinite cascade of sinks is formulated by the following theorem.

THEOREM 1.1 ([**Rob83**]). *Let $\{F_t : \mathrm{R}^2 \to \mathrm{R}^2\}$ be a one parameter family of C^1 diffeomorphisms depending continuously on t. Assume $\{F_t\}$ creates a homoclinic intersection at t_0 for the dissipative fixed point p_t. That is, there is some $\epsilon > 0$ such that for $t_0 - \epsilon < t < t_0 + \epsilon$ the subarcs $\gamma_t^s \subset W^s(p_t, F_t)$ and $\gamma_t^u \subset W^u(p_t, F_t)$ depending continuously on t satisfy the following condition:*

1. *$\gamma_t^s \cap \gamma_t^u = \emptyset$ for $t_0 - \epsilon < t < t_0$ (respectively, $t_0 < t < t_0 + \epsilon$),*
2. *for $t_0 < t < t_0 + \epsilon$ (respectively, $t_0 - \epsilon < t < t_0$), there are two transverse intersections of γ_t^s and γ_t^u and the directions at the two intersections are different from each other.*

Then there is a sequence of parameters t_j converging to t_0 such that F_{t_j} has a sink of period n_j and n_j diverges for $j \to \infty$. Moreover, $\{n_j\}$ satisfies $n_{j+1} - n_j = 1$ for all j if F_t preserves the orientations on $W^s(p_t, F_t)$ and $W^u(p_t, F_t)$. Otherwise, $n_{j+1} - n_j = 2$ for all j.

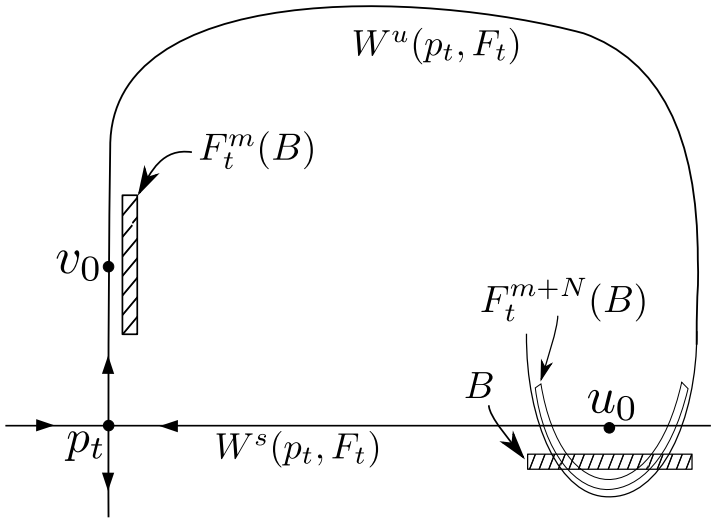

FIGURE 3. The situation of simple Newhouse sink. Perturbing the diffeomorphism F_{t_0} of a homoclinic tangency, we obtain the box B and the horseshoe region $F_t^{m+N}(B)$ near the point of the tangency u_0. The diffeomorphism F_t is linear in the neighborhood of the saddle fixed point p_t; F_t^m makes the box B shrink horizontally and stretch vertically. We obtain the rectangle $F_t^m(B)$ near v_0. F_t^N maps a neighborhood of v_0 to a neighborhood of u_0; this map is nonlinear and pulls the rectangle $F_t^m(B)$ across B. The $B \cap F_t^{m+N}(B)$ includes two saddle periodic points of period $m+N$. One of these two saddles becomes stable when the parameter varies to the homoclinic tangency.

Let us describe the situation of the theorem (Fig. 3). Let λ_t and μ_t be the two eigenvalues of $DF_t(p_t)$. We assume that $0 < \lambda_t < 1$ and $\mu_t < -1$. This settings are similar to the case of Hénon map (1) for the parameters $a \approx 1.3924198079$ and $b = -0.3$, which is numerically investigated in the following sections. We consider the case such that $\gamma_t^s \cap \gamma_t^u = \emptyset$ for $t_0 - \epsilon < t < t_0$ and there are transverse intersections of γ_t^s and γ_t^u for $t_0 < t < t_0 + \epsilon$. Let u_0 be the point of the tangency; $W^s(p_{t_0})$ is tangent to $W^u(p_{t_0})$ at u_0. We also let v_0 be $F_{t_0}^{-N}(u_0)$ for some integer $N > 0$. We consider sufficiently small neighborhood U of p_t and assume that F_t is linear in U. Transforming coordinate, we assume $F_t(x, y) = (\lambda_t x, \mu_t y)$ in U. We replace u_0 and v_0 by $F_{t_0}^{m_1}(u_0)$ and $F_{t_0}^{-m_2}(v_0)$ respectively for some integers m_1, m_2, if necessary, and we let u_0 and v_0 be in U, because u_0 and v_0 are a homoclinic point of F_{t_0}. Also we assume $p_t = (0, 0)$, $u_t = (x_0, 0)$, and $v_t = (0, y_0)$ for simplicity.

We take a box $B = \{(x, y) \mid |x - x_0| \le \delta^s, \delta_1^u \le y \le \delta_2^u\}$ near u_0 for $\delta^s, \delta_1^u, \delta_2^u \ge 0$. Because F_t is linear in U, the box B shrinks horizontally and stretches vertically by some iterations of F_t. We obtain a box $F_t^m(B)$ near v_0 for some integer m. Let N be an integer such that a neighborhood of v_0 is mapped to a neighborhood of u_0 by N iterations of F_t. Then $F_t^{m+N}(B)$ is a thin region having horseshoe shape parallel to $W^u(p_t, F_t)$. For suitable $\delta^s, \delta_1^u, \delta_2^u$ and m, $F_{t_1}^{m+N}(B) \cap B$ consists of two components for some parameter t_1. Two saddle periodic points of period $m+N$ exist in $F_{t_1}^{m+N}(B) \cap B$ (Fig. 4). When the parameter t approaches to t_0, $W^u(p_t, F_t)$ moves to the tangency point u_0. Eventually for the parameter t_2 smaller than t_1, $B \cap F_t^{m+N}(B)$ is the empty set. There is a parameter t between t_1 and t_2 such that one saddle periodic point of period $m+N$ becomes stable.

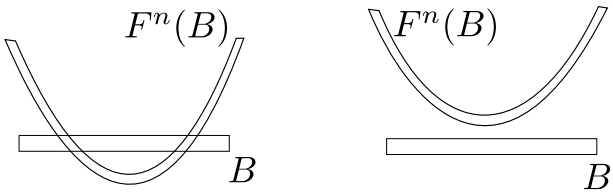

FIGURE 4. The left case is the situation such that each of two components of $F^n(B) \cap B$ includes one saddle periodic point. The right case is the situation such that no periodic point exists in $F^n(B) \cup B$. If F^n is dissipative, in the process of destruction of the horseshoe, that is, in the transformation from the left case to the right case, one of the two saddle periodic points obtains stability.

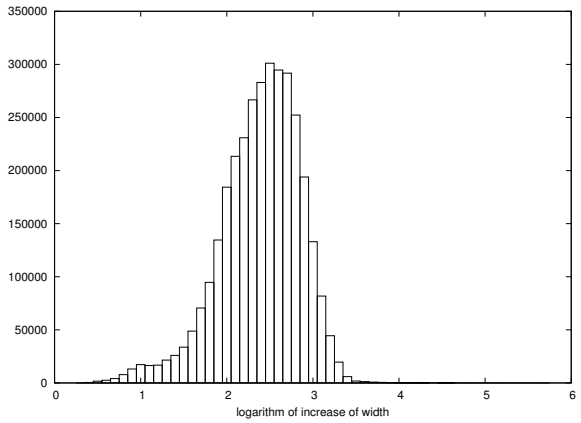

FIGURE 5. Distribution of increase ratios of widths of interval vectors after 10 iterations. The scale of x-axis is common logarithm. We calculate increases of width for 3312544 points except points that seem to diverge. Much of the increases of widths are less than 10^3 and the maximum increase of width is $10^{5.766122352727922}$.

To obtain a sink of period $m'+N$ higher than $m+N$, we take a suitable box B' closer to $W^s(p_t, F_t)$ than the box B, in which case $F_t^{m'}(B')$ is also closer to v_0 than $F_t^m(B')$. Similarly to the case of the box B, we obtain a sink of period $m'+N$ from the box B'. We remark that the above-mentioned two sinks that are constructed from B and B' do not coexist because the sink of period $m'+N$ exists at the parameter closer to the tangency than that of the sink of period $m+N$ Taking boxes closer to $W^s(p_t, F_t)$ in turn, we obtain a sequence of sinks approaching to the point of the tangency. If the eigenvalue μ_t is negative then there are two cascades of sinks for $t_0 > t$ and for $t_0 < t$ respectively. The periods of all sinks in the sequence for $t_0 > t$ are even and the periods for $t_0 < t$ are odd, or vice versa.

3. Computer program and precision

A feature of our numerical investigation is to use multiple precision library, in particular, MPFR[1] based on GMP[2] (The GNU Multiple Precision Arithmetic

[1]http://www.mpfr.org/
[2]http://gmplib.org/

Library). For interval arithmetic with multiple precision, we use MPFI[3]. Our computation can show finer structure of the system than computations with double precision.

To set suitable precision, we estimate errors when iterating points by Hénon map (1) whose parameters are $a = 1.4$ and $b = -0.3$ with interval arithmetic. We consider uniformly distributed points that seem to diverge. In particular, we collect points at a lattice of size 10^{-3} in $[-1, 1]\times[-1, 1]$ except points whose 10 times iteration goes out of $[-10, 10] \times [-10, 10]$. We take an interval vector with width 2^{-250} around each point and iterate it 10 times. Then, we calculate the ratio of the width of first interval vector and the width of iterated interval vector. Fig. 5 shows the distribution of the increase ratios of the widths for 3312544 points. Although the maximum increase of width is $10^{5.766122352727922}$, much of the increases of widths are less than 10^3. Roughly speaking, errors increases to about 1000 times when we carry out 10 iterations of points. The calculation in the following sections were usually carried out with precision from 256 bits to 1024 bits and we increased up to 12000 bits if needed.

The source code that we used to search for the cascade of sinks is available at the repository[4].

[3]http://mpfi.gforge.inria.fr/

[4]https://gitorious.org/math-numerical-experiment/math-henon-tangency/

CHAPTER 2

Basin of attraction of Newhouse sink

1. Settings and first sink in a sequence

We show locally and globally basins of attraction of the first few Newhouse sinks in this chapter. We deal with the Hénon map (1) of which parameter b is -0.3 and parameter a is varied in the neighborhood of 1.4. Then, the determinant of $DT(x, y)$ is -0.3 and the system is dissipative.

We sketch our procedure to obtain the first few sinks. Firstly, our investigation searches a parameter range including the parameter of a homoclinic tangency. We fix the value of the parameter a and calculate the stable and unstable manifolds of the fixed point (Fig. 2). We repeat the calculations with subtle changes of the parameter a and specify the parameter range that includes an occurrence of a homoclinic tangency (Fig. 1). Furthermore, we bisect the range of parameter a including the homoclinic tangency and obtain the narrower parameter range

$$[1.392419807923912503040934371 05, 1.392419807923912503040934371 06]. \tag{7}$$

Next, we seek coordinates of sinks and their parameters, by using the algorithm in Appendix 2, which is based on the proof of existences of Newhouse sinks. We obtained sinks of periods 13, 15, and 17 as a consequence of our computation. To obtain sinks of higher period we use the estimation in section 2.

Fig. 2 shows the orbit of the sink of period 13 and the stable and unstable manifolds of the saddle fixed point. The orbit starting from the point 0 in the figure goes to the saddle fixed point along the stable manifold and returns to the point 0 along the unstable manifold. The figure ensures that the situation of the sink is the same as that of the sink in Section . In the following sections, we focus on the basins of the sinks.

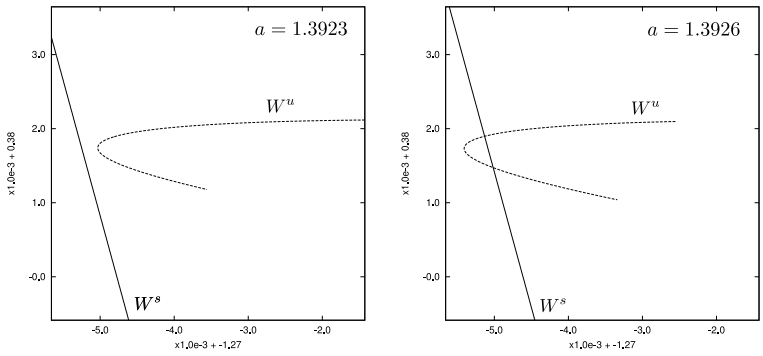

FIGURE 1. The segments of the stable and unstable manifolds for the saddle fixed point of Hénon map (1). The parameter b is constant and -0.3. The left image is the case that the parameter a is 1.3923 and the homoclinic tangency has not yet occurred. The right image is the case that the parameter a is 1.3926 and the two homoclinic points exist after the homoclinic tangency.

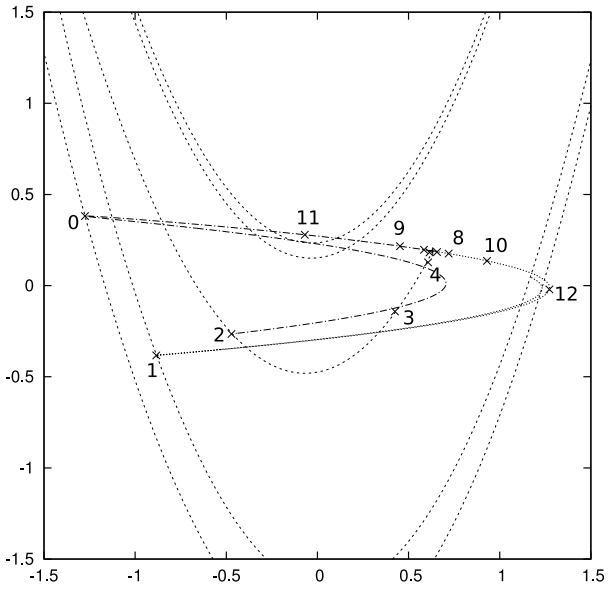

FIGURE 2. The orbit of the sink of period 13 and the stable and unstable manifolds for the saddle fixed point. The orbit starting from the point denoted by 0 moves along the stable manifold at first. After passing through the saddle fixed point the orbit moves along the unstable manifold with reversal because the eigenvalue of unstable direction for the saddle fixed point is negative.

2. Basin of attraction of a sink near a homoclinic tangency

Fig. 3, Fig. 4, and Fig. 5 show a neighborhood of the sink of period 13, which is displayed by 0 in Fig. 2. The scale of the main band of the basin of attractor as 10^{-7}. The basin of attraction of the sink of period 13 is parallel to the stable manifold of the saddle fixed point and the sink is nearly at the peak of the unstable manifold of the saddle fixed point. Similarly to [**GOY87**] the boundary of basin of the sink of period 13 consists of the stable manifold of the saddle fixed point of period 13, where both of the sink and the saddle are simultaneously born at the saddle-node bifurcation.

It is remarkable that the intersections of the basin of the sink of period 13 and the unstable manifold of the saddle fixed point in Fig. 4. The closure of the unstable manifold of the saddle fixed point includes Hénon attractor. Because there are the intersections of the basin of the sink of period 13 and the unstable manifold, Hénon attractor does not exist. Most points in the phase space get through the orbit like Hénon attractor and eventually converge to the sink. In other words, there are the chaotic transients like the Hénon attractor (Fig. 6). We discuss the transients in section 1. We note that the basin of attraction is large and covers most of phase space except points to diverge (Fig. 8) and a basin of attraction in this chapter is not correct. Because orbits with short transient are practically important, in this chapter, we regard a set of initial points of short transient orbits as a basin of attraction.

The basin of attractor that causes long chaotic transients is complicated. The outline of initial points of short transient orbits is shown in Fig. 9, which is calculated by iterating points backward in a small neighborhood. If we take points in a lattice and plot points that converges to the sink by iteration of fixed number, then

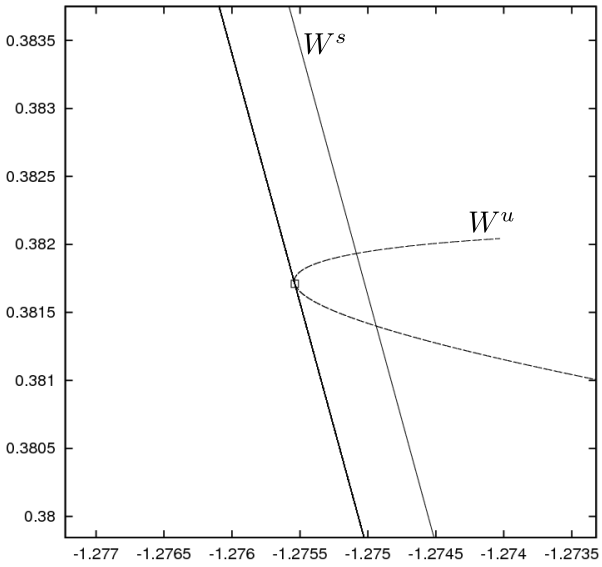

FIGURE 3. A neighborhood of the sink denoted by 0 in Fig. 2. There are the two vertical lines parallel to each other. The left thick one is the basin of attraction of the sink of period 13 denoted by the square. The right one is the stable manifold of the saddle fixed point. The curved line is the unstable manifold of the saddle fixed point. We observe that the position of the sink is near the peak of the curve of the unstable manifold and the basin of attraction is narrow and parallel to the stable manifold.

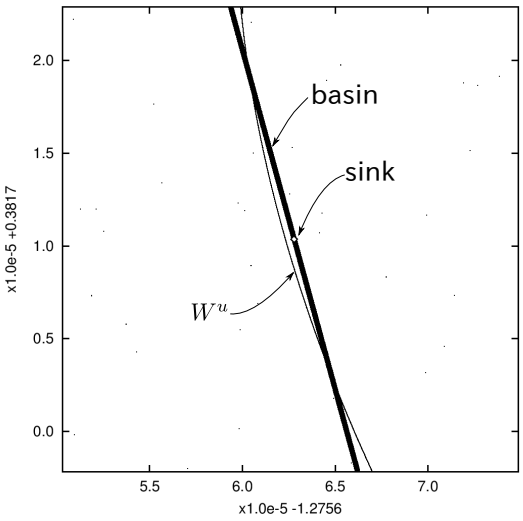

FIGURE 4. Magnification near the sink of period 13, where the sink is denoted by the diamond at the center. The thick line is the basin of attraction and the thin and curved line is unstable manifold of the saddle fixed point. There are two intersections of the basin and the unstable manifold.

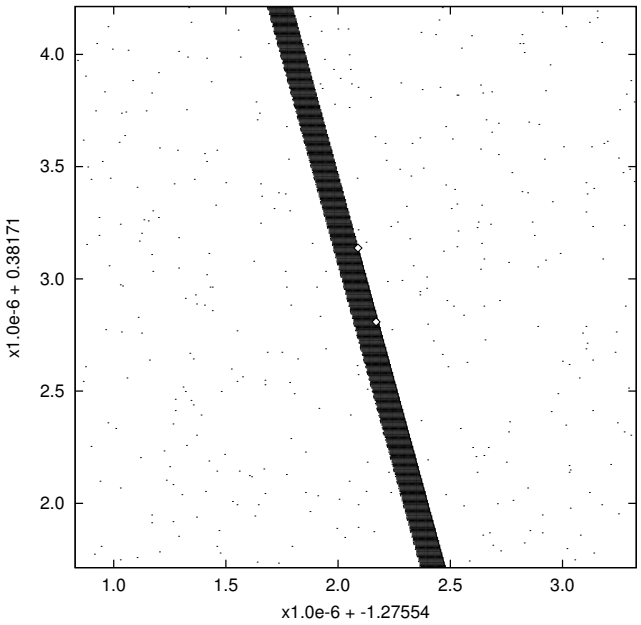

FIGURE 5. The points denoted by the diamonds are the periodic points of period 13. The upper one is a saddle and the lower one is a sink. The stable manifold of the saddle periodic point composes the boundary of basin of the sink.

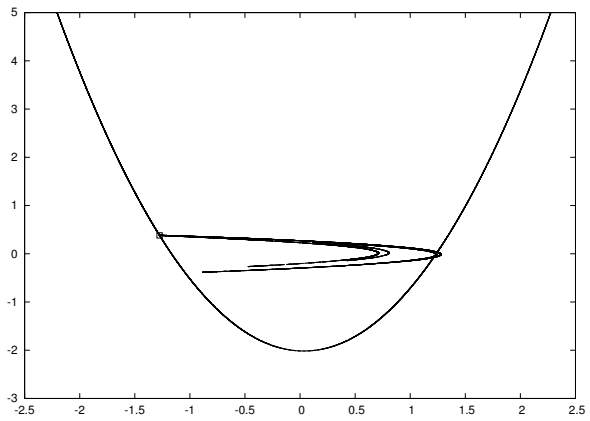

FIGURE 6. A chaotic transient and a stable manifold of a saddle of period 13 at $a = 1.3927060035$ and $b = -0.3$. $\square$ is the sink of period 13. The orbit like Hénon attractor is a long transient orbit. After sufficiently large iterations (about 1500000 iterations on the average), most orbits converge to the sink of period 13.

scattered points appear (Fig. 10). The procedure to calculate the points in Fig. 10 is the following. We iterate the points 1000×13 times with 12000 bit precision and we regard iterated points whose distance from the sink is less than 10^{-20} as points in the basin. The scattered points are not isolated points, but this means sensitive dependence on initial points of orbits. Actually, if we take points in a smaller lattice

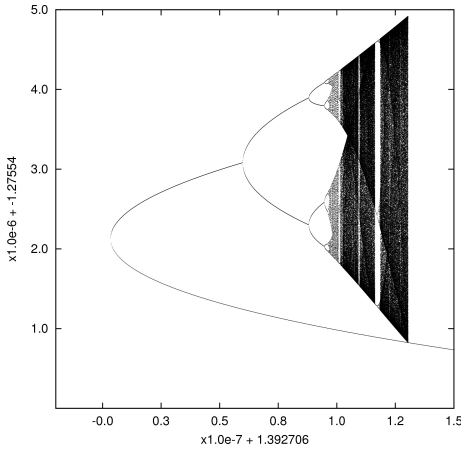

FIGURE 7. The vertical axis is x-coordinate of points in $\mathbb{R}^2$. The horizontal axis is the parameter a of (1). The lowest curve denotes the saddle fixed point of period 13. The upper curve and the following countless points denote the sink of period 13 denoted by 0 in Fig. 2 and the attractor arising from the sink by period-doubling bifurcation. The attractor collides with the saddle fixed point and then the attractor disappears, that is, the crisis occurs.

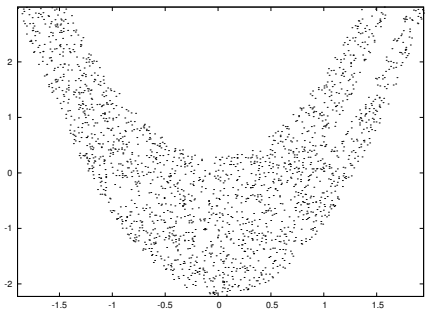

FIGURE 8. We plot points whose iterations approach to the sink of period 13. We test every point at a lattice of size 6×10^{-3} in the region $[-3, 3] \times [-3, 3]$.

in a neighborhood of a scattered point and plot points that converges by iteration of fixed number, we obtain a thick line of the basin of attraction (Fig. 11).

Let us mention the bifurcation of the sink of period 13. This sink is created through saddle-node bifurcation and proceeds to period-doubling bifurcation [**YA85**]. The period-doubling bifurcation is terminated by the crisis; the attractor arising from period-doubling bifurcation collides with the saddle periodic point of period 13. Fig. 7 shows the bifurcation diagram of the sink of period 13.

We show the movements of the stable and unstable manifolds, the sinks of period 13, 15, and 17, and their basins of attraction. Fig. 12 shows the region near the sink denoted by 0 in Fig. 2. When the parameter a decreases from about 1.3927 to the parameter value of the homoclinic tangency, the stable manifold moves to right and the unstable manifold moves to left; then these manifolds approaches to the tangency. In the next section, we estimate the position of the sink from the move of the stable and unstable manifolds.

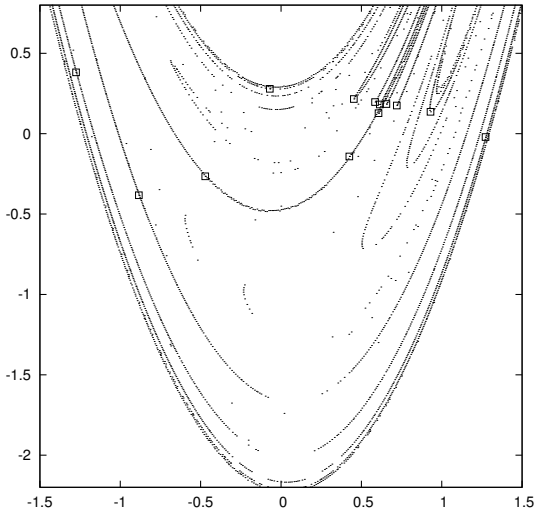

FIGURE 9. The main band of basin of attraction for the orbit of sink of period 13 denoted by □.

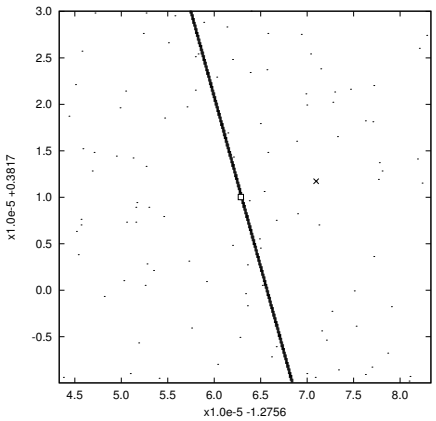

FIGURE 10. The basin of attraction near the sink of period 13 denoted by the square at the center. All scattered points apart from the central basin of attraction are also in the basin. There are scattered points around the basin that are in the basin of attraction. Because the basin bands around the scattered points are very narrow, the basins around these points are not displayed as lines. Actually, the scales of the basin bands are from 10^{-13} to 10^{-2201}.

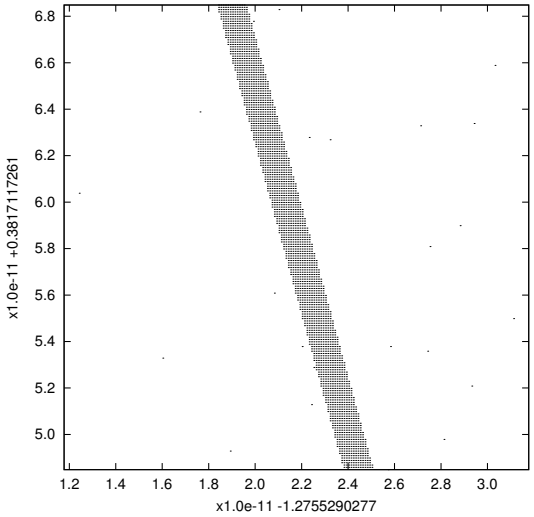

FIGURE 11. The basin of attraction around the scattered point $\times$ in Fig. 10. The scattered point is not displayed and its position is the center of the figure.

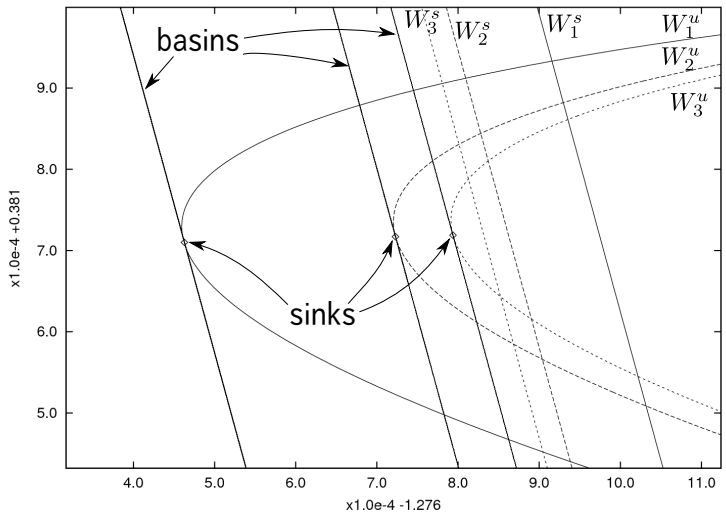

FIGURE 12. The movements of sinks, their basins of attraction, and the stable and unstable manifolds of the fixed points when the parameter a changes. The lines W_1^s and W_1^u are the stable and unstable manifolds of the fixed point for $a = 1.39270603828125$. Similarly, W_2^s and W_2^u are the stable and unstable manifolds for $a = 1.39249759364389038085937 5$, and W_2^s and W_2^u are the stable and unstable manifolds for $a = 1.39244095492362976074218 75$. When the parameter a increases, the stable manifold moves from left to right and the unstable manifold moves from right to left. The sinks exist near the peaks of the unstable manifolds and these basins are lines parallel to each stable manifold. Starting from the left of figure, the periods of the sinks are 13, 15, and 17, respectively.

CHAPTER 3

Estimation of sinks and power laws

1. Power laws of Newhouse sinks

In this chapter, we show an algorithm to obtain the succeeding sinks of a cascade from the first few sinks, the stable and unstable manifolds of the fixed point. The algorithm is derived from power laws of Newhouse sinks. We also shows numerical data of power laws of our obtained sinks. In this section, we recall the known results on the asymptotic behavior and the power laws of the parameter values of a cascade of sinks.

We consider the situation of Theorem 1.1 and for simplicity assume that the two eigenvalues λ_t and μ_t are positive. For the two-dimensional map

$$(x, y) \mapsto \left(\frac{(\mu - 1)}{\mu}, \frac{(1 - b)(\mu - 1)}{\mu} \right), \tag{8}$$

Curry and Johson observed numerically that a sequence of parameter values at saddle-node bifurcations approaches a parameter of a homoclinic tangency at a rate of an unstable eigenvalue at a fixed point [**CJ82**]. This phenomenon is formulated according to [**Rob83**, 5.3. Remark] by

$$\lim_{n\to\infty} \frac{t_n - t_{n-1}}{t_{n+1} - t_n} = \mu_{t_0}, \tag{9}$$

where t_n is the parameter value that the sink of period n exists and t_0 is the parameter of homoclinic tangency. This fact enables us to estimate the parameter value t_{n+1} from the last two parameter values t_{n-1} and t_n.

The relations of bifurcation parameters are described in [**TS94**] as

$$\lim_{n\to\infty} \frac{\bar{t}_n - t_0}{\bar{t}_{n+1} - t_0} = \lim_{n\to\infty} \frac{\tilde{t}_n - t_0}{\tilde{t}_{n+1} - t_0} = \mu_{t_0}, \tag{10}$$

where the saddle-node bifurcation creates the two periodic points of period n at $\bar{t}_n$, one of the periodic points changes its stability at $\tilde{t}_{n+1}$ through period-doubling bifurcation, and t_0 is the parameter of the homoclinic tangency.

We also are interested in the range of parameter such that a sink exists. The evaluation in [**TLY86**] gives

$$\lim_{n\to\infty} \frac{\bar{t}_n - \tilde{t}_n}{\bar{t}_{n+1} - \tilde{t}_{n+1}} = \mu_{t_0}^2. \tag{11}$$

This means that it becomes increasingly difficult to find sinks of higher period.

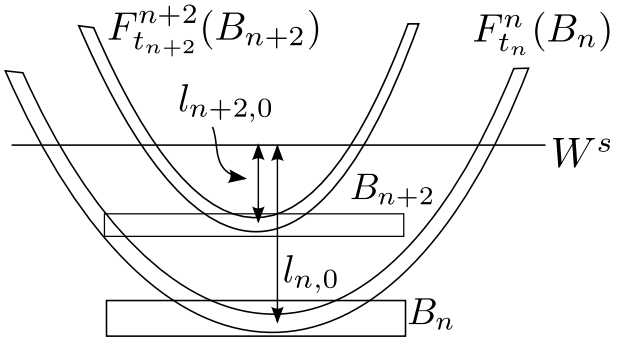

FIGURE 1. The situation that B_n and B_{n+2} include the sinks of period n and $n+2$ respectively. Then the relation (15) for $l_{n,0}$ and $n_{n+2,0}$ is satisfied. Note that the parameter t_n such that B_n includes a sink is different from the parameter t_{n+2} such that B_{n+2} includes a sink.

To apply these relations to our case such that the unstable eigenvalue is negative, we replace the diffeomorphism F_t by F_t^2;

$$\lim_{n\to\infty} \frac{t_n - t_{n-2}}{t_{n+2} - t_n} = \mu_{t_0}^2, \tag{12}$$

$$\lim_{n\to\infty} \frac{\bar{t}_n - t_0}{\bar{t}_{n+2} - t_0} = \lim_{n\to\infty} \frac{\tilde{t}_n - t_0}{\tilde{t}_{n+2} - t_0} = \mu_{t_0}^2, \tag{13}$$

$$\lim_{n\to\infty} \frac{\bar{t}_n - \tilde{t}_n}{\bar{t}_{n+2} - \tilde{t}_{n+2}} = \mu_{t_0}^4. \tag{14}$$

2. Estimation of positions of sinks

To find sinks numerically we want to estimate the positions of the sinks. In our case, because the unstable eigenvalue μ_t is negative, an infinite cascade of sinks is split into two sequences by the stable manifold: a sequence of even period on one side and a sequence of odd period on the other side. The estimation in such a situation is to obtain the approximate position of the sink of period $n+2$ from the position of the sink of period n for Hénon map $F_t = T_{t,-0.3}$.

The position of the box B in Fig. 3 relates to the position of stable manifold of the fixed point as below. Let B_n be the box including the sink of period n and $l_{n,i}$ be the distance between the stable manifold and the center point of $F_t^i(B_n)$ for an integer $i \geq 0$. The boxes B_n and B_{n+2} are mapped to a neighborhood of v_0 and F_t is approximately linear in the neighborhood of the saddle fixed point. We obtain $l_{n,i} = |\mu_t|^{-i} l_{n,0}$. Let k be an integer such that $F_t^k(B_n)$ is in a neighborhood of v_0. Then $F_t^{k+2}(B_{n+2})$ must be in a neighborhood of v_0 and $l_{n,k} = l_{n+2,k+2}$ holds. Therefore, we obtain the relation on the positions of two boxes including the sinks,

$$\frac{l_{n,0}}{l_{n+2,0}} = \mu_t^2. \tag{15}$$

The relation (15) does not take into account the condition that one of the two periodic points in the box is stable. We remember Fig. 4 and consider the intersection of the box and the horseshoe when the periodic point is stable. If the intersection of B_n and $F^n_{t_n}(B_n)$ is composed of two components, both of two periodic points of period n are saddle. If the intersection is empty then there is no periodic point. Therefore, at some parameter that the intersection is composed of one component, one of the two periodic points is stable. The horseshoe region created

by n iterations of the box B_n is narrow and is close to the unstable manifold of the fixed point. Consequently, the unstable manifold approximates to the horseshoe region and the sink is near the peak of the unstable manifold (Fig. 12). Let $\bar{l}$ be the distance between the stable manifold and the peak of the unstable manifold. We can regard $\bar{l}$ as $l_{n,0}$ for the parameters such that the sinks exist. We search for the parameter satisfying

$$\frac{l_{n,0}}{\bar{l}} = \mu_t^2 \tag{16}$$

and the obtained parameter is the estimation of parameter such that a sink exists. We can also regard the peak of the unstable manifold from the stable manifold as the estimation of position of the sink.

From the first three sinks of period 13, 15, and 17 mentioned in section 2. we obtained eventually the sinks of period 8 to 60. For example, the procedure to obtain the sink of period 19 from the two sinks of period of 15 and 17 is as below. We calculate the distance $l_{17,0}$ between the sink of period 17 and the stable manifold. Applying (12) to the two sinks of period 15 and 17, we obtain the first estimation of the parameter for the sink of period 19. To refine the estimation further, we search for the parameter such that the condition (16) holds from the calculations of the stable and unstable manifolds near the first estimation of parameter. We obtain the final estimation of the parameter in this way and also obtain the position of the peak of the unstable manifold at the parameter. The final estimation enables simple search to find the next sink. Fixing both a parameter in a neighborhood of the estimation of the parameter and an initial point in a neighborhood of the peak point of unstable manifold, we test convergences of iterations. If the convergent point is found then it is a sink of period 19. For the sinks of higher period, we repeat the above procedure.

3. Numerical data of power laws of obtained sinks

By using the estimation described in the last section, our computer program searched for sinks of odd period and sinks of even period, respectively. As a result, we obtained a sequence of sinks of period from 8 to 60. The numerical data of the sinks is listed in the tables in Appendix B: parameters values of sinks, coordinates of sinks, eigenvalues at sinks, parameter intervals where sinks persist, parameter intervals where attractors exist, lengths of these two types of parameter intervals, ratios of lengths of these two types of parameter intervals, distances between stable manifolds and peaks of unstable manifolds.

We make sure the known power laws of the cascade of sinks (12) and (15). We calculate the sizes of parameter intervals of periodic windows and the distances between stable manifolds and peaks of unstable manifolds. Fig. 2 shows that these values are governed by the power law. The shrinking ratio of the sizes of periodic windows is square of eigenvalue at the fixed point for unstable direction. The distances between the stable manifolds and the peaks of the unstable manifolds get smaller by absolute value of unstable eigenvalue at the fixed point. Because the sinks were obtained by the estimation derived from the power law of the distances, although it is trivial that the obtained sinks satisfy the power law, this data is for confirmation that the obtained sinks are a sequence of Newhouse sinks.

Our numerical data shows that the eigenvalues of Jacobian matrix of n-times composite at the sinks of period n exhibits the power laws shown in Fig. 3. The absolute values of one of the two eigenvalues are approximately constant. The absolute values of the other shrink at a rate of 0.3, which is the absolute value of the determinant of Jacobian matrix. Because the map (1) has the constant

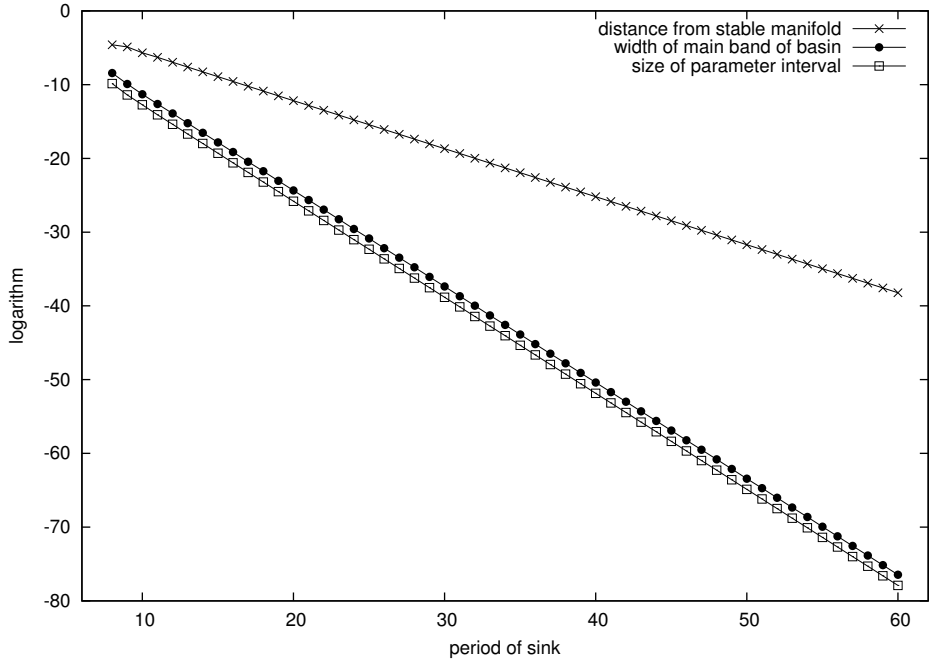

FIGURE 2. Logarithm of distance between peak of unstable manifold and stable manifold of a fixed point, logarithm of width of main band of basin, and logarithm of size of parameter interval that a sink exists. The slopes are about -0.650612, -1.30444, and -1.30478, which agree with $\log|\mu_{t_0}| \approx 0.65130925$ and $\log|\mu_{t_0}^2| \approx 1.3026185$.

determinant b at all of the domain, the determinant of n-times composite is equal to b^n.

We state other numerical data of the obtained sinks. In about 43% of the parameter intervals of periodic windows, the stable periodic point of minimum period, that is, the sink appeared by saddle-node bifurcation, exist (Appendix B Table 14). The lengths of the parameter intervals of the stable periodic points of minimum period in the periodic windows also satisfy the same power law as that of the lengths of the periodic windows (Appendix B Table 12).

We are interested in the properties of basins. As stated previously, the basins of the obtained sinks are most of phase space except points that go to infinity. However, in practice, there are points with long transients and points with short transients, of course, which is not rigorous distinction. The basins composing points with short transients are bands parallel to the stable manifolds shown in Fig. 12. For some parameter values we calculated such basins, but we could not observe radical change in neighborhoods of the sinks. As a sort of size of the basin, we consider width in a neighborhood of the sink. We calculate two basin boundaries in a neighborhood of the sink and we regard minimum distance between the two boundaries as the width of the basin. The calculated result is shown in Fig. 2; the shrinking ratio of the widths of basins is the square of eigenvalue.

We describe the difficulty of finding sinks of high period in the cascade of sinks. For example, for the sink of period 27, the size of parameter interval is about 6.6×10^{-15} and the width of the basin of attraction is about 7.9×10^{-14}. It seems to be difficult for the calculation with double precision (53 bit) to find the sink of

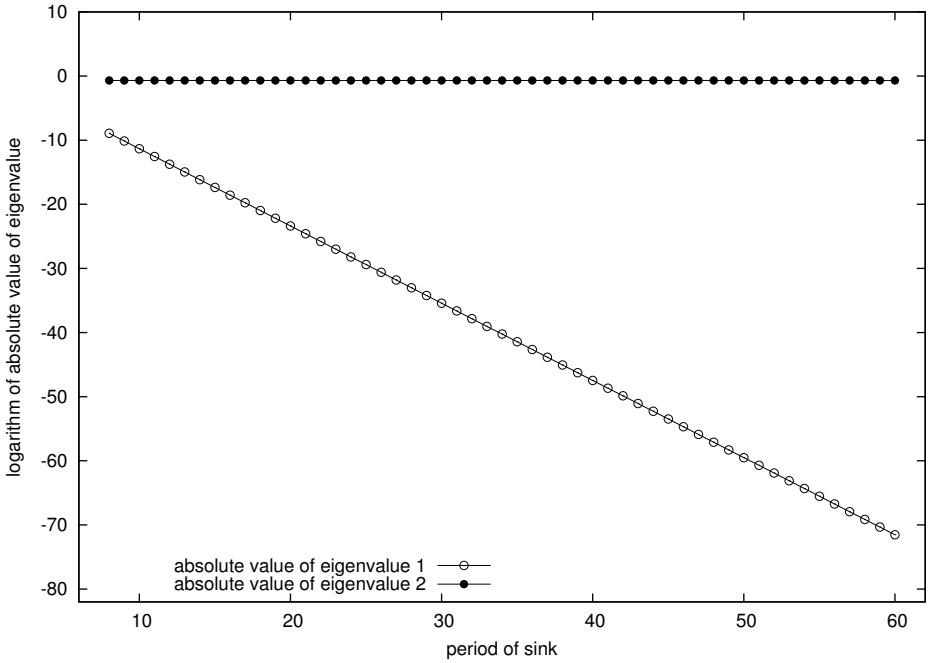

FIGURE 3. Logarithm of absolute value of eigenvalue. The slope of logarithm of the absolute value of one eigenvalue are approximately one, that is, the value are approximately constant. The other slope is approximately 0.3, which is the absolute value of the determinant.

period larger than 27. Even if the precision is sufficient large, it is difficult that numerical investigation finds the sinks of higher period. There are two reasons; the basin of attraction is narrow and the parameter interval that a sink exists is short. The width of the basin of the sink of period $n+2$ is about 7% of that of the sink of period n. The size of the parameter interval of the sink of period n is about 7.4% of that of the sink of period n. If we search for the sink of period $n+2$ in the same region to the region of period n with finer step, we must calculate about 200 ($\approx 1/(0.07 \times 0.074)$) times as much as the case of period n. Therefore, to obtain a sequence of sinks, we need the above mentioned estimations of positions and parameter values of sinks.

CHAPTER 4

Verification of sinks

1. Interval arithmetic

Interval arithmetic is a method that defines operations on a set of intervals and deals with rounding errors on computers nicely. We consider an interval enclosing a number instead of the number itself. When some arithmetic operations produce a resultant number, we calculate intervals enclosing the number instead of calculating the approximation of the number. In implementations of interval arithmetic on computers, endpoint numbers of intervals are numbers that is represented rigorously by floating point numbers and rounding errors of digital computation are brought into extra expansions of resultant intervals. It is mathematically rigorous that the interval calculated by interval arithmetic on computers is an interval enclosing true value. In this section, we recall definitions of interval arithmetic and fundamental theorems according to [**Moo79**].

For a closed interval X in $\mathbb{R}$, we will denote the endpoints of X by $\underline{X}$ and $\overline{X}$, that is, $X = [\underline{X}, \overline{X}]$. Identifying $x \in \mathbb{R}$ with $[x, x]$, we regard x as an interval. Replacing elements of usual vector and matrix by intervals, we define an n-dimensional-interval vector and a matrix. We call two intersections X and Y equal if $\underline{X} = \underline{Y}$ and $\overline{X} = \overline{Y}$. We also call two interval vector or two interval matrices are equal if all elements are equal. The intersection and union of two intervals are the usual intersection and union of two sets in $\mathbb{R}$. If $X \cap Y \neq \emptyset$ then we have

$$X \cap Y := \{\max(\underline{X}, \underline{Y}), \min(\overline{X}, \overline{Y})\} \tag{17}$$

$$X \cup Y := \{\min(\underline{X}, \underline{Y}), \max(\overline{X}, \overline{Y})\}. \tag{18}$$

The intersection of two interval is an interval except an empty set, but the union is not always an interval. The intersection and union of two interval vectors or two interval matrices are these of two sets in $\mathbb{R}^n$ for some integer n.

We define the width of an interval X by

$$w(X) := \overline{X} - \underline{X}. \tag{19}$$

and the absolute value of X by

$$|X| := \max(|\underline{X}|, |\overline{X}|). \tag{20}$$

For an n-dimensional interval vector $V = (V_1, V_2, \ldots, V_n)$, we define the width of V by

$$w(V) := \max(w(V_1), w(V_2), \ldots, w(V_n)) \tag{21}$$

For an interval matrix M, we define the width of M by

$$w(M) := \max_{i,j}(M_{ij}). \tag{22}$$

For two intervals X and Y, we define arithmetic operations by

$$X \circ Y := \{x \circ y \mid x \in X, y \in Y\}, \tag{23}$$

where $\circ$ is the addition $+$, the subtraction $-$, or the product $\cdot$. We will sometimes omit the dot to express the product of two intervals. Before defining the quotient

of two intervals, we need to define the reciprocal of an interval. For an interval X with $0 \notin X$,

$$1/X := \{1/x \mid x \in X\}. \tag{24}$$

We define the quotient of two intervals X and Y with $0 \notin Y$ by

$$X/Y := X \cdot (1/Y). \tag{25}$$

From these definitions, we have

$$X + Y = [\underline{X} + \underline{Y}, \overline{X} + \overline{Y}], \tag{26}$$

$$X - Y = [\underline{X} - \overline{Y}, \overline{X} - \underline{Y}], \tag{27}$$

$$X \cdot Y = [\min(\underline{X} \cdot \underline{Y}, \underline{X} \cdot \overline{Y}, \overline{X} \cdot \underline{Y}, \overline{X} \cdot \overline{Y}), \max(\underline{X} \cdot \underline{Y}, \underline{X} \cdot \overline{Y}, \overline{X} \cdot \underline{Y}, \overline{X} \cdot \overline{Y})]. \tag{28}$$

We remark that addition and multiplication are associative and commutative, however, the distributive law does not always hold. Alternatively, we have

$$X(Y + Z) \subset XY + XZ. \tag{29}$$

We deal with extension of a real valued function f of n real variables to an interval valued function of n interval variables. Of course, for a real vector valued function, we consider each element of the function as a real valued function. If an interval valued function F of n interval variables satisfies

$$F(Y_1, Y_2, \ldots, Y_n) \subset F(X_1, X_2, \ldots, X_n) \tag{30}$$

for $Y_i \subset X_i$ where $i = 1, 2, \ldots, n$, then F is called inclusion monotonic. Arithmetic operations $+$, $-$, $\cdot$, and $/$ are inclusion monotonic. We define an interval extension of f as an interval valued function F of n interval variables so that

$$F(x_1, \ldots, x_n) = f(x_1, \ldots, x_n). \tag{31}$$

From the following theorem, calculating the functions by interval arithmetic, we can obtain bounds of values of functions.

THEOREM 4.1 ([**Moo79**, Theorem 3.1]). *If F is an inclusion monotonic interval extension of f, then $f(X_1, \ldots, X_n) \subset F(X_1, \ldots, X_n)$.*

If we replace real variables of a rational function, then we obtain the interval extension of the rational function. Because rational interval functions are inclusion monotonic, we have the following corollary.

COROLLARY 4.2 ([**Moo79**, Corollary 3.1]). *If F is a rational interval function and an interval extension of f, then $f(X_1, \ldots, X_n) \subset F(X_1, \ldots, X_n)$.*

We remark that if we have two different expressions of a real rational function then two different interval extensions obtained by replacing real variables by intervals does not always coincide.

We calculate bounds of eigenvalues in section 3. To do so, we need to extend square root function to an interval valued function. Because square root is monotonic increasing function, we simply define

$$\sqrt{X} := [\sqrt{\underline{X}}, \sqrt{\overline{X}}]. \tag{32}$$

Simple iterations of interval extension of Hénon mapping produce interval vectors with too large widths. We need to refine the bounds. We introduce some definitions and state theorem that subdividing interval vectors at each iteration step produces refined bounds. For an interval extension $F(X)$, if there is a constant L such that $w(F(X)) \leq Lw(X)$ for any $X \subset X_0$ then $F(X)$ is said to be

Lipschitz in X_0. For an inclusion monotonic interval extension $F(X)$ of a real valued function $f(x)$, we define the excess width of $F(X)$ by

$$w(E(X)) = w(F(X)) - w(f(X)), \tag{33}$$

where $E(X) := F(X) - f(X)$. A uniform subdivision of an interval vector $X = (X_1, X_2, \ldots, X_n)$ means that X is expressed by the union of interval vectors $(X_{1,j_1}, \ldots, X_{n,j_n})$ for a positive integer N;

$$X = \bigcup_{1 \le i_k \le N, 1 \le k \le n} (X_{1,j_1}, \ldots, X_{n,j_n}), \tag{34}$$

where

$$X_{i,j} := \left[\underline{X}_i + (j-1)\frac{w(X_i)}{N}, \underline{X}_i + j\frac{w(X_i)}{N} \right], \tag{35}$$

for $1 \le i \le n, 1 \le j \le N$. Obviously,

$$X_i = \bigcup_{j=1}^{N} X_{i,j} \tag{36}$$

$$w(X_{i,j}) = \frac{w(X)}{N}. \tag{37}$$

The following theorem guarantees that we can obtain arbitrarily refined bounds of a function by using a uniform subdivision of the argument of the function.

THEOREM 4.3 ([**Moo79**, Theorem 4.1]). *We suppose that $F(X)$ is an inclusion monotonic interval extension of a real valued function f and Lipschitz in X_0. For a positive integer N we take a uniform subdivision $\{X_{i,j}\}$ of $X \subset X_0$. We consider*

$$F_{(N)}(X) := \bigcup_{1 \le i_k \le N, 1 \le k \le n} F(X_{1,j_1}, \ldots, X_{n,j_n}) \tag{38}$$

and define E_N by

$$E_N = F_{(N)}(X) - f(X_1, \ldots, X_n). \tag{39}$$

Then, there is a constant K such that

$$w(E_N) \le K\frac{w(X)}{N}. \tag{40}$$

2. Application of Brouwer fixed point theorem with interval arithmetic

In this section we show how to verify the existences of the obtained sinks. The way is a direct application of Brouwer fixed point theorem. To construct numerically an inclusion required by the theorem, we use interval arithmetic. We also check that the periodic points are sinks by calculating enclosures of eigenvalues at the periodic points.

Before applying fixed point theorem, we extend the map (1) to an interval valued map. Just replacing real numbers by intervals, we obtain the interval extension $\bar{T}$ of Hénon map;

$$\bar{T}_{A,B}(X, Y) = (1 + Y - AX^2, -BX), \tag{41}$$

where A, B, X, and Y are intervals. Practically, we take very small intervals A and B that include the specified parameters a and b in (1).

From Brouwer fixed point theorem, if we construct a rectangle that is mapped back into itself by n iterations and has no intersections with its images of m iterations for $0 < m < n$, an existence of a periodic point of period n is guaranteed. Taking a rectangle is convenient to test numerically that the rectangle includes its image. However, our sinks do not have such rectangle neighborhoods because parts

of the rectangle are away from the sinks transiently. In general, points sufficiently close to a sink approach monotonically to the sink in two directions of eigenvectors at the sink, but points in a rectangle neighborhood do not always approach monotonically to the sink in the distance of the orthogonal coordinate.

To construct an inclusion on a rectangle including the obtained sink of period n, we consider coordinate change from the orthogonal coordinate to the coordinate of the eigenvectors at the sink. We take a small rectangle R around the origin and map R to a neighborhood of the sink by a linear transform g, which maps the origin to the sink and x-axis and y-axis to the eigendirections of the sink. After iterating R by $T_{a,b}$, we restore the coordinate by g^{-1} and we check

$$g^{-1} \circ T_{a,b}^n \circ g(R) \subset R. \tag{42}$$

Because the linear transform g is a homeomorphism, if $g^{-1} \circ T_{a,b}^n \circ g$ has a periodic point in R then $T_{a,b}$ has a periodic point of period n in $g(R)$.

We extend the linear transform g and its inverse g^{-1} to interval extensions $\bar{g}$ and $\bar{g}^{-1}$ by replacing real variables by intervals. From Corollary 4.2 we obtain the following relation;

$$g^{-1} \circ T_{a,b}^n \circ g(R) \subset \bar{g}^{-1} \circ \bar{T}_{A,B}^n \circ \bar{g}(R), \tag{43}$$

where A and B are intervals satisfying $a \in A$ and $b \in B$. Therefore, if we find a rectangle R such that

$$\bar{g}^{-1} \circ \bar{T}_{A,B}^n \circ \bar{g}(R) \subset R, \tag{44}$$

then Hénon map $T_{a,b}$ has periodic points in $g(R)$.

However, in our case, size of a rectangle increases approximately twofold at each iteration of $\bar{T}_{A,B}$ and $\bar{g}^{-1} \circ \bar{T}_{A,B} \circ \bar{g}(R)$ become too large rectangle so that R can not include it. From Theorem 4.3, the following procedure produces finer enclosure of $g^{-1} \circ T_{a,b} \circ g(R)$. We take appropriate threshold value L of maximum width and subdivide R into interval vectors whose width are less than L. We let the set of the subdivided interval vectors S_R. We map each interval vector in S_R by $\bar{g}$ and let S_0 be the set of obtained interval vectors. If there are interval vectors in S_0 whose widths are larger than L, we subdivide them and replace them in S_0 by the subdivided interval vectors. Thus, the widths of all interval vectors in S_0 are less than L. We map each interval vector in S_0 and obtain the set of interval vectors S_1. Similarly, we repeat mapping with subdivision n times and obtain S_n. We let S be the set obtained by mapping all interval vectors in S_n by $\bar{g}^{-1}$. If all interval vectors in S are included in R, we obtain an existence of a periodic point of period n. This procedure causes increase of amount of computation. For that reason, the verification for sinks of high period are very hard and we constructed only inclusions for the sinks of period 8 to 14.

In implementations of interval arithmetic on computers, because there are rounding errors on computations we can not always obtain exact endpoints of intervals. We extend intervals a bit so that they are expressed by floating point numbers on computers at each calculation. Although the sets $S_0, \ldots, S_n$ and S are expanded a bit by rounding errors, if we take the parameters A and B and the rectangle R and so on whose endpoints are exact floating point number on computers, then A, B, and R have no errors. Therefore, the above-mentioned algorithm is valid even if there are extra expansions of intervals at each mapping step.

3. Result of verification of sinks

By using the way stated in the last section, we could verify the existences of the sinks of period from 8 to 14, whose data is shown in Table 1. Fig 1 shows a neighborhood of the sink of period 13. The left figure is the region enclosing the

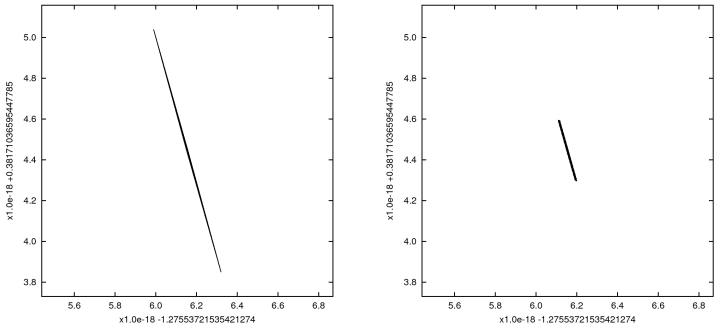

FIGURE 1. Regions such that the iteration of 13 times maps the region in the left figure to the region in the right figure. The regions are composed small rectangle regions. The iteration for each small rectangle region are calculated by interval arithmetic. From this data of the two regions, we obtained that the iteration of 13 times of Hénon map is an inclusion on the region in the left figure and a periodic point of period 13 exists.

sink of period 13, the right figure is the region mapped by 13 iterations of the map. The former covers the latter, which is tested through transformation by coordinate change as stated in the last section. Both regions are stretched thin regions. The two directions of the eigenvectors are close to each other and the region is stretching in the directions of eigenvectors at the sink of period 13.

Table 1 shows the numerical data obtained from the verification. We state the verification of the sinks of period 8 to 14 as a proposition.

PROPOSITION 4.4. *Hénon map (1) has the periodic points of period 8 to 14 in the ranges of parameter a, x-coordinate and y-coordinate listed in Table 1, when $b = -0.3$. The absolute values of the eigenvalues at the periodic points are less than one. Therefore, the periodic points are stable.*

We note the difference of the values in Table 1 and the values shown in Appendix B; the former are rigorous bounds obtained by interval arithmetic and the latter are approximate values obtained by usual computation.

8	x	$[-1.2641480315599056, -1.2641480315599057]$
	y	$[0.3815883095535991, 0.3815883095535990]$
	a	$[1.3866414978735625, 1.3866414978735626]$
	α	$[-0.0001317565296413, -0.0001317565296411]$
	β	$[-0.4979639352876563, -0.4979639352876542]$
9	x	$[-1.2797615433863033, -1.2797615433863034]$
	y	$[0.3815001609062766, 0.3815001609062765]$
	a	$[1.3968296778150859, 1.3968296778150860]$
	α	$[0.0000393390430422, 0.0000393390430427]$
	β	$[-0.5003426234527945, -0.5003426234527932]$
10	x	$[-1.2725951827993173, -1.2725951827993174]$
	y	$[0.3817739305802194, 0.3817739305802193]$
	a	$[1.3904445108073844, 1.3904445108073845]$
	α	$[-0.0000118133309073, -0.0000118133309067]$
	β	$[-0.4998505541313075, -0.4998505541313065]$
11	x	$[-1.2764873308253127, -1.2764873308253128]$
	y	$[0.3816834340024865, 0.3816834340024864]$
	a	$[1.3934818331832507, 1.3934818331832508]$
	α	$[0.0000035426394508, 0.0000035426394519]$
	β	$[-0.5000424187451586, -0.5000424187451572]$
12	x	$[-1.2744909451906007, -1.2744909451906008]$
	y	$[0.3817369729481438, 0.3817369729481437]$
	a	$[1.3918712413591354, 1.3918712413591355]$
	α	$[-0.0000010629383349, -0.0000010629383331]$
	β	$[-0.4999735008295995, -0.4999735008295976]$
13	x	$[-1.2755371627643452, -1.2755371627643453]$
	y	$[0.3817101619053220, 0.3817101619053219]$
	a	$[1.3927060351470881, 1.3927060351470882]$
	α	$[0.0000003188573829, 0.0000003188573864]$
	β	$[-0.5000113143693783, -0.5000113143693747]$
14	x	$[-1.2749930656059051, -1.2749930656059052]$
	y	$[0.3817242881938740, 0.3817242881938739]$
	a	$[1.3922705183540199, 1.3922705183540200]$
	α	$[-0.0000000956602776, -0.0000000956602712]$
	β	$[-0.4999953250901844, -0.4999953250901780]$

TABLE 1. The data of verified periodic points: the ranges of x-coordinate, y-coordinate, parameter a, and two eigenvalues, where α and β are two eigenvalues at the periodic points. The ranges of x-coordinate and y-coordinate are coordinates of four corners of minimum rectangles that include images of inclusions obtained by our numerical construction. When the parameter b is -0.3 and the parameter a is in the specified range, a periodic point exists in the ranges of x-coordinate and y-coordinate and the periodic points are sinks because the absolute values of the eigenvalues are less than one.

CHAPTER 5

Chaotic transients

1. Chaotic transients

The appearances of simple Newhouse sinks found by our computer program cause chaotic transients, which are chaotic behaviors before the orbits converge to a periodic attractor. In our case, chaotic transients are orbits like the Hénon attractor before they converge to simple Newhouse sinks, which is shown in Fig. 6. In this section, we investigate these chaotic transients. At the beginning, we review known results related to chaotic transients. Subsequently, we show the analysis for average rambling times of our cascade of sinks.

Firstly, we review influence of simple Newhouse sinks to a chaotic attractor. Tatjer and Simó proved under some conditions that when a simple Newhouse sink exists the closure of the unstable manifold of the saddle fixed point includes the

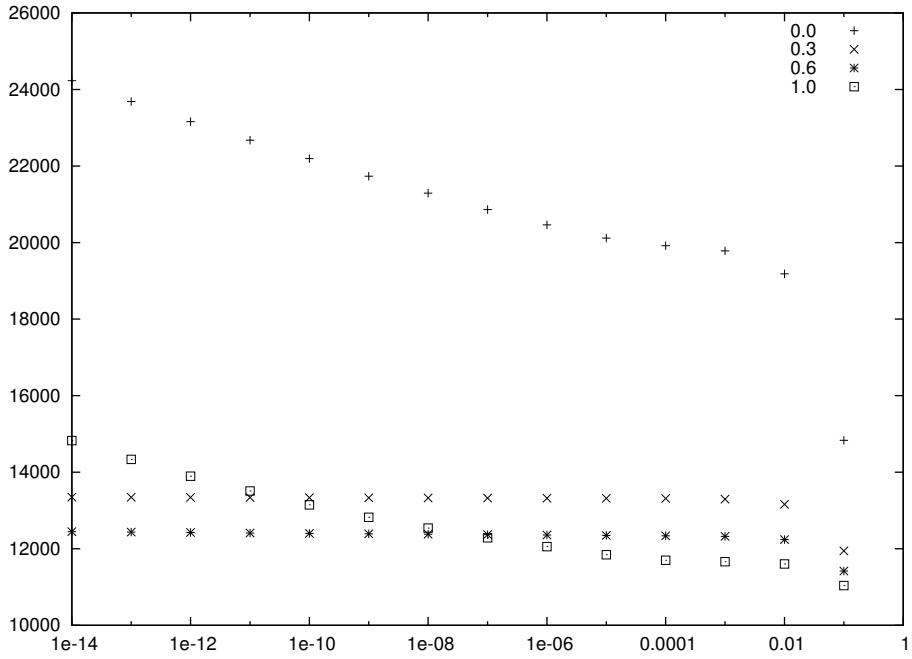

FIGURE 1. Relation of average rambling time and various threshold values for parameters where the sink of period 8 exists. The horizontal axis means threshold values with log scale and the vertical axis means average rambling time. The numbers 0.0, 0.3, 0.6, and 1.0 on the horizontal axis are fractions in the parameter interval. The number 0.0 means a parameter just after saddle-node bifurcation and the number 1.0 means a parameter just before period-doubling bifurcation.

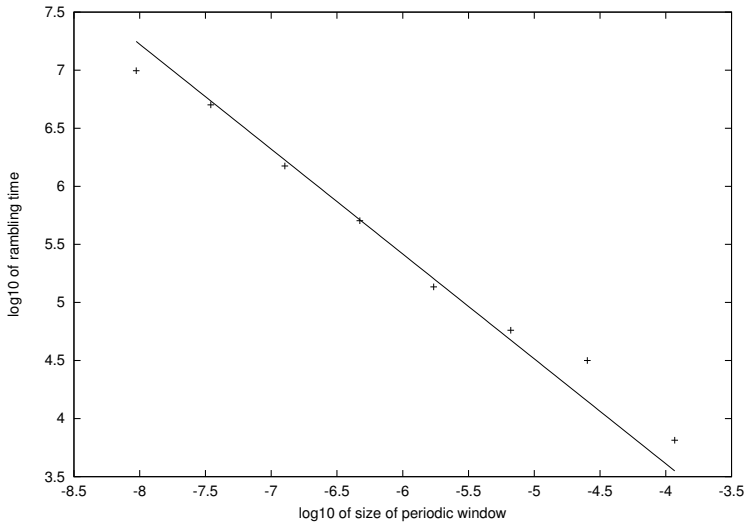

FIGURE 2. Logarithms to base 10 of average rambling time and size of periodic window. Average rambling time is calculated at a center of parameter interval from saddle-node bifurcation to period-doubling bifurcation. The points from left to right corresponds to sinks of periods 15, 14, 13, 12, 11, 10, 9, and 8. We can seem to fit the relation with linear mapping. The slope of the linear mapping is -0.902897.

sink [**TS94**]. In that case, a chaotic attractor does not exist in the closure of the unstable manifold of the saddle fixed point. In particular, the Hénon attractor does not exist. The numerical investigation in this paper seems to give a specific case of [**TS94**, Theorem 5.8], but it is not clear that the condition of the theorem holds because it is difficult to calculate numerically some of values in the condition.

Secondly, we review studies of rambling time, which is an iteration number needed for an orbit to enter a neighborhood of a periodic point. To begin with, we need to define a suitable neighborhood of a periodic point to determine rambling time. For example, Jacobs et al. considered a quadratic map $y = a - x^2$ and defined an immediate basin as below. Let x_s and x_u be two fixed points; $x_s = (-1 + \sqrt{1+4a})/2$ and $x_u = (-1 - \sqrt{1+4a})/2$. For a parameter a such that x_s is stable, an immediate basin is defined as an interval $[x_u, -x_u]$. Buszko and Stefański also defined a black subset as a union of intervals whose orbits monotonically approach a periodic point [**BS03**].

Because rambling time depends on its initial point, we take a lot of uniformly distributed initial points in phase space and we consider the average of rambling time. For one-dimensional quadratic maps, Jacobs et al. showed numerically in [**JOH97**] that, for a given parameter where a periodic point is stable, the average rambling time scales with the size of periodic window including the parameter;

$$\tau \sim \triangle a^{-1/2},$$

where τ is the average rambling time and $\triangle a$ is the size of the periodic window of parameter space. Moreover, for Hénon map with small b, they approximated Hénon map by a logistic map and conjectured

$$\tau \sim \triangle a^{1/2-d}, \tag{45}$$

where d is a fractal dimension of Hénon attractor. In [**BS06**], for Hénon map with $b = -0.3$, the average rambling time for windows of low period exhibits the same type scaling as (45),

$$\tau \sim \triangle a^{-\beta}, \tag{46}$$

where β is a constant determined by numerical calculation and $\beta = 0.9 \pm 0.1$.

In the rest of this section, we apply the same analysis in [**BS06**] and investigate the same type scaling of average rambling time for the obtained sinks. First of all, we state the definition of rambling time at an initial point and how to determine a threshold value that is required to calculate rambling time. In our numerical investigation, the definition of the rambling time of an initial point for a stable periodic point is simply the minimum number of iterations that the distance from the sink becomes less than an appropriate threshold value. In other word, we take an appropriate threshold distance d for a stable periodic point p_N of period N, and define the rambling time for an initial point q as the integer $r_d(q)$ such that for all integers $i >= r_d(q)$ and $k < r_d(q)$,

$$\max\{|T^i(q) - T^j(p_N)| \mid 0 \leq j < N\} \leq d$$
$$\max\{|T^k(q) - T^j(p_N)| \mid 0 \leq j < N\} > d.$$

If the threshold value is too large, we may obtain a number of iterations that do not make orbits converge to periodic points. On the contrary, too small threshold value causes an overestimation of rambling time. When Lyapunov multiplier of the sink has an absolute value near one, in particular, at parameters near saddle-node bifurcation and period-doubling bifurcation, the rate of convergence of orbits is slow and therefore the overestimation of rambling time is large.

How to determine the appropriate threshold value is the following. Let α and β be eigenvalues of $DT^N(p_N)$ and let Lyapunov multiplier $|\Lambda|$ be $\max\{|\alpha|, |\beta|\}$, where $DT^N(p_N)$ is the Jacobian matrix of Nth iteration of Hénon map T at the stable periodic point p_N. Obviously, $|\Lambda|$ is less than one because p_N is stable. For sufficient small threshold values d_0 and d_1 such that $d_1 < d_0$, we denote rambling times for some initial point q by r_0 and r_1 respectively. Then, because the distance from the orbit of the stable periodic point decreases approximately at the rate $|\Lambda|^{1/N}$ at every iteration in the neighborhood of the periodic point, we have

$$\frac{d_1}{d_0} \approx |\Lambda|^{\frac{(r_0 - r_1)}{N}}.$$

Therefore,

$$\frac{r_0 - r_1}{\log d_0 - \log d_1} \approx -\frac{N}{\log |\Lambda|}.$$

We take about 10000 uniformly distributed initial points in $[-1.5, 1.5] \times [-1.0, 1.0]$ and calculate averages of all values of rambling time. For various threshold values, we calculate values of average rambling time. The result shown as the graph in Fig. 1, which is the relation between logarithms of threshold distance and average rambling time. As stated above, for sufficient small thresholds, the rate of contraction is constant and the graph has the constant slope whose absolute value is almost $N/\log|\Lambda|$. Therefore, the threshold value at the change of the slope is appropriate. From the graph we take 10^{-6} as the appropriate threshold value for the sink of period 8.

We calculated average rambling time for the sinks of period from 8 to 15. Each parameter is at the middle value of the parameter interval when each sink persists. We plot the sizes of parameter intervals of the periodic windows and the logarithms

of values of average rambling time and obtain Fig. 2. From (46) we consider fitting

$$\log \tau = -\beta \log \triangle a + \gamma$$

for some constants β and γ with the graph in 2. Our obtained fitting parameter β is is -0.902897 and this value agrees with the value for the case of large periodic window, that is, the case of sinks of lower period, investigated in [**BS06**]. As for average rambling time, the sinks that we obtained have the same scaling property as that of the sinks of lower period.

Bibliography

[AM06] Zin Arai and Konstantin Mischaikow, *Rigorous computations of homoclinic tangencies*, SIAM J. Appl. Dyn. Syst. **5** (2006), 280–292.

[BS03] Katarzyna Buszko and Krzysztof Stefański, *Transient dynamics inside periodic windows and in their vicinity i. logistic maps*, Open Syst. Inf. Dyn. **10** (2003), 183–203, 10.1023/A:1024614307468.

[BS06] ———, *Measuring transient chaos in nonlinear one- and two-dimensional maps*, Chaos, Solitons & Fractals **27** (2006), no. 3, 630 – 646.

[CJ82] J.H. Curry and J.R. Johnson, *On the rate of approach to homoclinic tangency*, Physical letters **92** (1982), no. 5, 217–220.

[FG92] John Erik Fornæss and Estela A. Gavosto, *Existence of generic homoclinic tangencies for Hénon mappings*, J. Geom. Anal. **2** (1992), no. 5, 429–444. MR MR1184708 (93j:58089)

[GOY87] Celso Grebogi, Edward Ott, and James A. Yorke, *Basin boundary metamorphoses: changes in accessible boundary orbits*, Physica D **24** (1987), 243–262.

[GS72] N. K. Gavrilov and L. P. Silnikov, *On three-dimensional dynamical systems close to systems with a structurally unstable homoclinic curve. i*, Mathematics of the USSR - Sbornik **17** (1972), 467–485.

[Hén76] M. Hénon, *A two-dimensional mapping with a strange attractor*, Comm. Math. Phys. **50** (1976), no. 1, 69–77.

[JOH97] Joeri Jacobs, Edward Ott, and Brian R. Hunt, *Scaling of the durations of chaotic transients in windows of attracting periodicity*, Phys. Rev. E **56** (1997), no. 6, 6508–6515.

[Moo79] Ramon E. Moore, *Methods and applications of interval analysis*, SIAM Studies in Applied Mathematics, 1979.

[New74] Sheldon E. Newhouse, *Diffeomorphisms with infinitely many sinks*, Topology **13** (1974), 9–18.

[New79] ———, *The abundance of wild hyperbolic sets and non-smooth stable sets for diffeomorphisms*, Publications mathématiques de l'I.H.É.S. **50** (1979), 101–151.

[Rob83] Clark Robinson, *Bifurcation to infinitely many sinks*, Comm. Math. Phys. **90** (1983), no. 3, 433–459.

[TLY86] Laura Tedeschini-Lalli and James A. Yorke, *How often do simple dynamical processes have infinitely many coexisting sinks?*, Comm. Math. Phys. **106** (1986), no. 4, 635–657.

[TS94] J. C. Tatjer and C. Simó, *Basins of attraction near homoclinic tangencies*, Ergodic Theory Dynam. Systems **14** (1994), no. 2, 351–390. MR MR1279475 (95b:58097)

[YA85] James A. Yorke and Kathleen T. Alligood, *Period doubling cascades of attractors: a prerequisite for horseshoes*, Comm. Math. Phys. **101** (1985), no. 3, 305–321. MR MR815187 (87k:58210)

APPENDIX A

Algorithm

1. Calculation of stable and unstable manifolds

We show the algorithm to compute a stable manifold of a saddle fixed point of a two-dimensional diffeomorphism. Let $f : \mathbb{R}^2 \to \mathbb{R}^2$ be a diffeomorphism that has a saddle fixed point p. If we want to obtain manifolds of a saddle periodic point of period n, we can apply this algorithm by replacing f with f^n. To obtain an unstable manifold, we replace f with f^{-1}. We assume that the two eigenvalues of f are positive by replacing f by f^2 if needed.

The algorithm uses the following facts; on a neighborhood of a saddle fixed point, the stable and unstable manifolds approximate the eigenvectors of Jacobian matrix of the diffeomorphism at the saddle fixed point and the diffeomorphism in the neighborhood approximates a linear map.

Firstly, in advance, we obtain numerically the saddle fixed point p by some way and calculate the eigenvectors of Jacobian matrix. Let $v_s, v_u \in \mathbb{R}^2$ be the eigenvectors of Jacobian matrix at p with the eigenvalues whose absolute values are less than 1 and larger than 1, respectively. We take a sufficiently small neighborhood U of p such that $f|_U$ approximates a linear map.

We consider calculation of a first point on the stable manifold near $p+c_1v_s \in U$ for small $c_1 \in \mathbb{R}$. We take $c_2 \in \mathbb{R}$ such that $q = p + c_1v_s + c_2v_u \in U$. Because $f|_U$ is nearly a linear map, in the neighborhood U, some iterations of f maps q to the positive direction of v_s or the negative direction v_u. Varying the value of c_2, we search for a pair (c_-, c_+) of c_2, so that $f^{l_1}(c_-)$ is mapped to the negative direction of v_u and $f^{l_2}(c_+)$ is mapped to the positive direction of v_u for suitable iteration numbers l_1 and l_2. We apply bisection method to the pair (c_-, c_+) and then we obtain small interval $[c'_-, c'_+]$ (or $[c'_+, c'_-]$) of c_2 such that the point on the stable manifold is $p + c_1v_s + c'_2v_u$ for some c'_2 in the interval. In practice, we define the point on the stable manifold as $p + c_1v_s + ((c'_- + c'_+)/2)v_u$.

We let q_1 be the first point of the stable manifold in the above-mentioned way and let q_0 be $f(q_1)$. Secondly, we calculate the segment of the stable manifold between between q_0 and q_1, that is, we calculate sufficiently many points on the stable manifold between q_0 and q_1. Finally, to stretch the stable manifold distant from the fixed point, we iterate the points by f^{-1} a number of times.

2. Search for a sink near a homoclinic tangency

We show the algorithm to search for a sink near a parameter value that a homoclinic tangency occurs. Here, we search for a sink when two transversal homoclinic points exists after the homoclinic tangency. Let f be the diffeomorphism of surfaces that satisfies such a condition. Note that sinks may exist before the homoclinic tangency occurs, that is, at parameters such that there is no homoclinic point near the tangency. In that case, the same algorithm can find sinks by determining suitable search region at the opposite side.

In advance, we find the search region like the Fig. 1, in which the unstable manifold stick a little out of the stable manifold. We take a parallelogram so

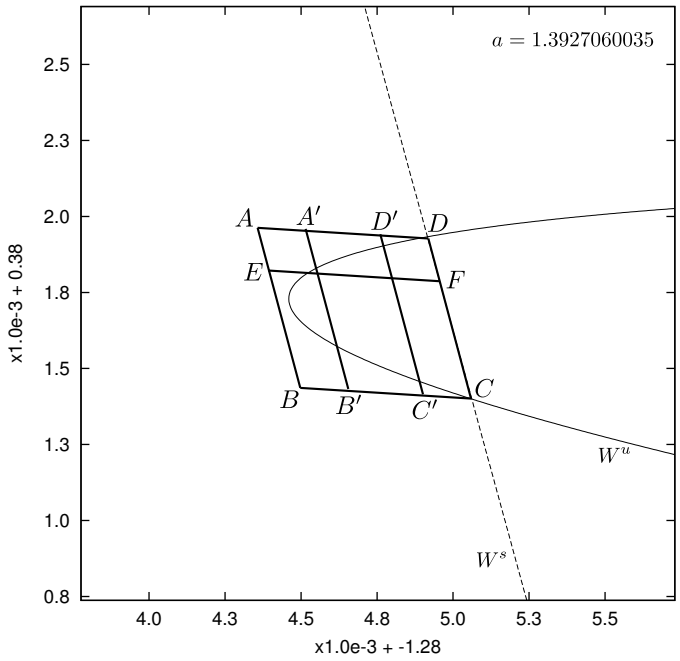

FIGURE 1. The parameters of map (1) are $a = 1.3927060035$ and $b = -0.3$. The points D and C are homoclinic points: the intersections of the stable and unstable manifolds for the saddle periodic point. The parallelogram $ABCD$ includes the segment of the unstable manifold from D to C. The lines AD, EF, and BE are parallel to each other. The lines AB, DC, $B'C'$, and $D'E'$ are parallel to each other. In $ABCD$ there is a periodic saddle point of period 13.

that its two vertexes are homoclinic points and it includes the curve of unstable manifold between the two homoclinic points. Here we fix the parameter value near the tangency and let this parallelogram be $ABCD$, where C and D are the homoclinic points. If we find a period m of periodic point and a parallelogram $A'B'C'D'$ satisfying the following conditions:

(1) A' and D' are on AD and B' and C' are on BC,
(2) $A'B'$ is parallel to AB and $C'D'$ is parallel to CD,
(3) the intersection of the parallelogram $A'B'C'D'$ and the region $f^m(A'B'C'D')$ has two components; that is, there is a horseshoe,

we proceed to the next step, where we calculate approximate coordinates of two saddle periodic points of period m in the intersection of $A'B'C'D'$ and $f^m(A'B'C'D')$. If we can not obtain m and $A'B'C'D'$ satisfying the conditions, We repeat perturbing the parameter and trying to find them until they are found.

We want to obtain two periodic points of period m in $ABCD$. We fix the line segment EF parallel to AD and map the line m times. $f^m(EF)$ is alike the shape of the unstable manifold. Then we calculate the point of the intersection of EF and $f^m(EF)$ and let q be the intersection point. We determine whether $f^m(q)$ is on the AD side from EF or the BC side from EF. To change the position of line EF and repeat this procedure, we divide AB and CD with sufficiently small size and then obtain points $E_1, \ldots, E_k$ and $F_1, \ldots, F_k$ such that E_iF_i is parallel to AD for all i. For E_iF_i we calculate the intersection q_i by the above procedure. Then we pick up a pair of points (q_-, q_+) from q_i so that q_- and q_+ are mapped to the different side

from EF. We shorten the distance of two points q_- and q_+ by bisection method and obtain a sufficiently short line segment between q_- and q_+. Then the midpoint of q_- and q_+ approximates point of periodic point. In the case that the condition (3) is satisfied, we obtain two saddle periodic points.

One of the two saddle periodic points becomes a sink when the intersection of a suitable parallelogram $A'B'C'D'$ and $f^m(A'B'C'D')$ consists of one component at a parameter nearer to the tangency. Although there is not necessarily a periodic point in such a case, if we find a pair of (q_-, q_+) then we obtain approximate coordinate of a periodic point. We repeat searching for periodic points until we take suitable parameter and the obtained periodic point is a sink.

3. Pseudo code of search for periodic points in a horseshoe

The algorithm in Appendix 2 to search for periodic points in the search region $ABCD$ is expressed by the following pseudo code.

```
def q_and_direction(EF)
  q = (an intersection of EF and f^m(EF))
  tmp, distance_q = projection(DA, DC, q - D)
  tmp, distance_fq = projection(DA, DC, f^m(q) - D)
  return [q, distance_fq - distance_q]
end

def calc_periodic_point
  n = (sufficient large number of partition of AB and DC)
  error = (maximum distance of coordinates of periodic points)
  vector_step = (B - A) / n
  q_interval_data = []
  last = nil
  for i from 0 to n
    E = A + vector_step * i
    F = E + (D - A)
    q, direction = q_and_direction(EF)
    current = [E, q, direction]
    if last
      E_last, q_last, direction_last = last
      if direction > 0 && direction_last < 0
        q_interval_data.push [current, direction_last]
      else if direction < 0 && direction_last > 0
        q_interval_data.push [direction_last, current]
      end
    end
    last = current
  end
  if q_interval_data.empty?
    return nil
  end
  periodic_points = []
  for data_plus, data_minus in q_interval_data
    E_plus, q_plus, direction_plus = data_plus
    E_minus, q_minus, direction_minus = data_minus
    while (q_plus - q_minus).abs > error
      E = (E_plus + E_minus) / 2
      F = E + (D - A)
```

```
      q, direction = q_and_direction(EF)
      if direction > 0
        E_plus, q_plus = E, q
      else
        E_minus, q_minus = E, q
      end
    end
    periodic_points.push ((q_plus + q_minus) / 2)
  end
  return periodic_points
end
```

APPENDIX B

Numerical data of sinks

1. Data tables

Numerical data of the obtained sinks are listed in the following tables. Table 1 shows the list of the values of the parameter a where the sinks exist. Table 2 and 3 show the list of the coordinates of the sinks. Table 4 and 5 show the list of the eigenvalues of the sinks. Table 8 and 9 show the list of the parameter intervals where the sinks of specified period exist, that is, the parameter intervals between saddle-node bifurcation and period-doubling bifurcation. Table 10 and 11 show the list of the parameter intervals where the attractor arising from the saddle-node bifurcations exist, that is, the parameter intervals of periodic windows. Table 12 shows the list of ratios of lengths of the parameter intervals where the sinks exist. Table 13 shows the list of ratios of lengths of the parameter intervals where the attractors arising from the saddle-node bifurcations exists. Table 14 shows the list of ratios of lengths of the parameter intervals in Table 12 and 13. Table 15 shows the list of the distances between the stable manifolds and the peak of the unstable manifolds and their ratios.

period	parameter a	period	parameter a
		8	1.38664149787356250000
9	1.39682967781508590995	10	1.39044451080738447805
11	1.39348183318325079174	12	1.39187124135913547473
13	1.39270603514708815022	14	1.39227051835401997070
15	1.39249759396078376854	16	1.39237923569364948177
17	1.39244095493338897575	18	1.39240878086818029898
19	1.39242555647987797736	20	1.39241681068117711904
21	1.39242137052683480445	22	1.39241899322602361400
23	1.39242023267157798334	24	1.39241958647359244535
25	1.39241992337792816159	26	1.39241974772878703645
27	1.39241983930576794529	28	1.39241979156096093336
29	1.39241981645332931688	30	1.39241980347537751260
31	1.39241981024159838398	32	1.39241980671394307857
33	1.39241980855313113200	34	1.39241980759424702657
35	1.39241980809417346952	36	1.39241980783353045237
37	1.39241980796942000901	38	1.39241980789857225808
39	1.39241980793550963533	40	1.39241980791625186329
41	1.39241980792629214800	42	1.39241980792105751770
43	1.39241980792378665887	44	1.39241980792236378636
45	1.39241980792310561907	46	1.39241980792271885514
47	1.39241980792292049944	48	1.39241980792281536962
49	1.39241980792287018039	50	1.39241980792284160409
51	1.39241980792285650271	52	1.39241980792284873513
53	1.39241980792285278485	54	1.39241980792285067348
55	1.39241980792285177427	56	1.39241980792285120036
57	1.39241980792285149957	58	1.39241980792285134357
59	1.39241980792285142491	60	1.39241980792285138250

TABLE 1. The values of parameter a where the sink exists.

period	x coordinate	y coordinate
9	-1.27976154338630332676	0.38150016090627654680
11	-1.27648733082531270876	0.38168343400248646793
13	-1.27553716276434521174	0.38171016190532197212
15	-1.27527703273885344572	0.38171694500136863446
17	-1.27520623128411636160	0.38171877870769113704
19	-1.27518697955868689668	0.38171927701715012326
21	-1.27518174604472220710	0.38171941247399922304
23	-1.27518032343168631819	0.38171944929478208728
25	-1.27517993673462261571	0.38171945930346351249
27	-1.27517983162267160731	0.38171946202402293808
29	-1.27517980305121079612	0.38171946276352383767
31	-1.27517979528493993763	0.38171946296453424263
33	-1.27517979317391901322	0.38171946301917274315
35	-1.27517979260010318583	0.38171946303402452279
37	-1.27517979244412908254	0.38171946303806152270
39	-1.27517979240173234159	0.38171946303915885577
41	-1.27517979239020809754	0.38171946303945713191
43	-1.27517979238707558788	0.38171946303953820909
45	-1.27517979238622411191	0.38171946303956024741
47	-1.27517979238599266448	0.38171946303956623785
49	-1.27517979238592975265	0.38171946303956786617
51	-1.27517979238591265201	0.38171946303956830877
53	-1.27517979238590800373	0.38171946303956842908
55	-1.27517979238590674024	0.38171946303956846178
57	-1.27517979238590639680	0.38171946303956847067
59	-1.27517979238590630344	0.38171946303956847309

TABLE 2. The coordinates of sinks of odd period.

period	x	y
8	-1.26414803155990566355	0.38158830955359902274
10	-1.27259518279931735196	0.38177393058021936800
12	-1.27449094519060074464	0.38173697294814371573
14	-1.27499306560590518015	0.38172428819387392387
16	-1.27512906462917220609	0.38172077592692207224
18	-1.27516600565582752278	0.38171981987086304374
20	-1.27517604505617454618	0.38171956002976662202
22	-1.27517877380397668935	0.38171948940301306126
24	-1.27517951551703021723	0.38171947020562793720
26	-1.27517971712775127688	0.38171946498743782459
28	-1.27517977192930977783	0.38171946356903620597
30	-1.27517978682541319353	0.38171946318348788627
32	-1.27517979087445722178	0.38171946307868536363
34	-1.27517979197506578554	0.38171946305020205462
36	-1.27517979227423197757	0.38171946304245888379
38	-1.27517979235555106303	0.38171946304035414230
40	-1.27517979237765514390	0.38171946303978203373
42	-1.27517979238366345528	0.38171946303962652358
44	-1.27517979238529662910	0.38171946303958425299
46	-1.27517979238574055693	0.38171946303957276302
48	-1.27517979238586122500	0.38171946303956963983
50	-1.27517979238589402489	0.38171946303956879089
52	-1.27517979238590294052	0.38171946303956856013
54	-1.27517979238590536396	0.38171946303956849741
56	-1.27517979238590602270	0.38171946303956848036
58	-1.27517979238590620176	0.38171946303956847572
60	-1.27517979238590625043	0.38171946303956847446

TABLE 3. The coordinates of sinks of even period.

period	two eigenvalues	
9	3.9339043042486357269 3e-05	-5.0034262345279381969 0e-01
11	3.5426394513598529461 7e-06	-5.0004241874515789171 3e-01
13	3.1885738465954306107 8e-07	-5.0001131436937652084 4e-01
15	2.8697845599296212023 5e-08	-4.9999944944828519116 3e-01
17	2.5828078201790783014 5e-09	-4.9999911720511246065 7e-01
19	2.3245337275852539932 8e-10	-4.9999767833326617167 5e-01
21	2.0920753418704102718 1e-11	-4.9999887640987009849 8e-01
23	1.8828734170284932825 4e-12	-4.9999738684278924799 8e-01
25	1.6945827215428585618 0e-13	-4.9999837639768522134 3e-01
27	1.5251226130521608943 4e-14	-4.9999897842483803373 8e-01
29	1.3726151295372885879 1e-15	-4.9999723803145345487 5e-01
31	1.2353501165408381409 7e-16	-4.9999865464336804832 8e-01
33	1.1118188309121467772 0e-17	-4.9999697900374800001 6e-01
35	1.0006335048184168432 7e-18	-4.9999869940472202377 5e-01
37	9.0057338851950722495 3e-20	-4.9999690378508648428 9e-01
39	8.1051464165142430958 9e-21	-4.9999777237359852088 8e-01
41	7.2946128073707723391 0e-22	-4.9999907247053596969 0e-01
43	6.5651699318862851294 4e-23	-4.9999767073846824330 4e-01
45	5.9086283777442479877 4e-24	-4.9999749125990749627 e-01
47	5.3177833662998572613 5e-25	-4.9999807302150681027 2e-01
49	4.7860164484175798875 2e-26	-4.9999688009793205268 7e-01
51	4.3073954037538106448 0e-27	-4.9999913200414703098 9e-01
53	3.8766715687480449283 7e-28	-4.9999710638215759474 7e-01
55	3.4889884786460552643 0e-29	-4.9999938972804327869 0e-01
57	3.1400984305655507358 0e-30	-4.9999798853417068886 9e-01
59	2.8260815922194837003 9e-31	-4.9999922615968540696 7e-01

TABLE 4. The eigenvalues of Jacobian matrix at sinks of odd period.

period	two eigenvalues	
8	-1.3175652964124709 1095e-04	-4.9796393528765527 0780e-01
10	-1.1813330906999108 4047e-05	-4.9985055413130701 2274e-01
12	-1.0629383339680761 5975e-06	-4.9997350082959852 5112e-01
14	-9.5660274406312188 2799e-08	-4.9999532509018116 8966e-01
16	-8.6023920630560781 9397e-09	-5.0040408161433251 3694e-01
18	-7.7484168766548100 2823e-10	-4.9999954205775689 4204e-01
20	-6.9735963546281603 8970e-11	-4.9999802450365928 4505e-01
22	-6.2762342056048456 7082e-12	-4.9999822474718791 0007e-01
24	-5.6485970233126712 3535e-13	-4.9999944289771024 0236e-01
26	-5.0837371341365510 8715e-14	-4.9999946127441225 2093e-01
28	-4.5753772197196747 3237e-15	-4.9999795331329250 7077e-01
30	-4.1178436641398275 0698e-16	-4.9999744742047511 6763e-01
32	-3.7090117209315485 7698e-17	-4.9959944272876006 1741e-01
34	-3.3354364293248404 8777e-18	-4.9999998659972561 5837e-01
36	-3.0018982290464217 0476e-19	-4.9999908006434298 0871e-01
38	-2.7017182240018567 8205e-20	-4.9999726310172888 8163e-01
40	-2.4315369686447897 2700e-21	-4.9999920280187923 1238e-01
42	-2.1883921984454351 2559e-22	-4.9999716325638595 2844e-01
44	-1.9695426629989365 4582e-23	-4.9999978202256538 7678e-01
46	-1.7725959708470903 4774e-24	-4.9999764556708708 4226e-01
48	-1.5953301693111338 2843e-25	-4.9999959012444295 5948e-01
50	-1.4358025626914180 8060e-26	-4.9999770605378341 3257e-01
52	-1.2922225696447730 1264e-27	-4.9999760420550460 7867e-01
54	-1.1629951664938145 1037e-28	-4.9999981666604230 0859e-01
56	-1.0466999389861197 6437e-29	-4.9999776777889028 2377e-01
58	-9.4203060505690475 6496e-31	-4.9999741748960719 7743e-01
60	-8.4782359710125519 9667e-32	-4.9999974546772887 8269e-01

TABLE 5. The eigenvalues of Jacobian matrix at sinks of even period.

period	ratios of eigenvalues of period $n-2$ and n	
11	9.005403226341284300 89e-02	9.994000017316848649 35e-01
13	8.998544364311577494 13e-02	1.000161763461898969 86e+00
15	9.002229444468103479 35e-02	9.997523452960340308 20e-01
17	9.000005980387668060 43e-02	9.999993355129228699 88e-01
19	9.000025899813494672 49e-02	9.999971222512264982 26e-01
21	8.999978434572667914 59e-02	1.000002396164334043 69e+00
23	9.000026812347585067 86e-02	9.999970208591436324 77e-01
25	8.999982187954033121 66e-02	1.000001979120135450 80e+00
27	8.999989163489108756 14e-02	1.000001204058215448 20e+00
29	9.000031327253972199 78e-02	9.999965192061190571 28e-01
31	8.999974500916926596 80e-02	1.000002833239479823 56e+00
33	9.000030161695397607 13e-02	9.999966487117425476 09e-01
35	8.999969032701915729 01e-02	1.000003440822737472 71e+00
37	9.000032321353587424 75e-02	9.999964087513873990 54e-01
39	8.999984365337126965 64e-02	1.000001737187781486 63e+00
41	8.999976598211714225 27e-02	1.000002600205459470 27e+00
43	9.000025231294759643 50e-02	9.999971965306639464 07e-01
45	8.999962589005823994 00e-02	1.000004156794409535 27e+00
47	9.000030169996984779 04e-02	9.999966477893501562 40e-01
49	9.000021472758331442 78e-02	9.999976141436554971 02e-01
51	8.999959465617763039 20e-02	1.000004503840533039 39e+00
53	9.000036461406820607 03e-02	9.999959487489881893 60e-01
55	8.999958899723892997 17e-02	1.000004566718200042 42e+00
57	9.000025221591171354 38e-02	9.999971976088343788 78e-01
59	8.999977722706256938 10e-02	1.000002475260987241 98e+00

TABLE 6. The ratios of absolute values of eigenvalues of at sinks of odd periods $n-2$ and n. The absolute value of one eigenvalue shrinks at a rate of square of the determinant at the saddle fixed point, that is, 0.09. The absolute value of the other eigenvalue are approximately constant.

period	ratios of eigenvalues of period $n-2$ and n	
10	7.4920691480608615454 6e-02	1.2012702795634807232 7e+00
12	8.9977868421370580979 9e-02	1.0002459669140613089 3e+00
14	8.9996071596365258657 6e-02	1.0000436508345870954 9e+00
16	8.9926483239195530683 3e-02	1.0008175206919737094 7e+00
18	9.0072817186875743297 4e-02	9.9919157422683174070 0e-01
20	9.0000273160816826134 0e-02	9.9999696488902496954 6e-01
22	8.9999963956036873115 8e-02	1.0000004004886395786 9e+00
24	8.9999780732661671886 2e-02	1.0000024363096947917 3e+00
26	8.9999996692190073862 0e-02	1.0000000367534449745 7e+00
28	9.0000271434112635283 5e-02	9.9999698407451099750 5e-01
30	9.0000091061172012023 0e-02	9.9999898821022358599 9e-01
32	9.0071698283045928835 9e-02	9.9920398655279463622 0e-01
34	8.9927902101293937012 4e-02	1.0008017300195088794 3e+00
36	9.0000163176669098366 4e-02	9.9999818692918613877 6e-01
38	9.0000327055060769548 3e-02	9.9999636606808584749 7e-01
40	8.9999650853416260245 6e-02	1.0000038794215358503 4e+00
42	9.0000367120271642283 2e-02	9.9999592090250974550 5e-01
44	8.9999528621882202144 3e-02	1.0000052375620741112 0e+00
46	9.0000384563796953942 6e-02	9.9999572708718059594 7e-01
48	8.9999649979389013304 2e-02	1.0000038891330251490 4e+00
50	9.0000339134274629256 8e-02	9.9999623185559197404 1e-01
52	9.0000018332778028107 5e-02	9.9999796302507847038 0e-01
54	8.9999601756957192315 1e-02	1.0000044249422778906 9e+00
56	9.0000368801333855572 1e-02	9.9999590222419344012 4e-01
58	9.0000063052396622173 5e-02	9.9999929941830612423 9e-01
60	8.9999580963724781002 4e-02	1.0000046559802915960 4e+00

TABLE 7. The ratios of absolute values of eigenvalues of at sinks of even periods $n-2$ and n. The absolute value of one eigenvalue shrinks at a rate of square of the determinant at the saddle fixed point, that is, 0.09. The absolute value of the other eigenvalue are approximately constant.

period	parameters at saddle-node and period-doubling bifurcations
9	1.396823348997703097450000000000000000000
	1.396834598750085909950000000000000000000
11	1.393481403358592016170307617187500000000
	1.393482167476929332991596679687500000000
13	1.392706003390799087717650465878906250000
	1.392706059846112759592650465878906250000
15	1.392497591610285308212949204559529708211 8
	1.392497595788962077349576401825154708211 8
17	1.392440954759597090716292662765449605723 9
	1.392440955068561007758259853114074788829 4
19	1.392425556467034236291927218379247459980 1
	1.392425556489867630446008146112743351268 0
21	1.392421370525885764036147874351071633486 3
	1.392421370527572949574533121099857840912 3
23	1.392420232671507861403381837340262099177 3
	1.392420232671632523034864262849448755130 8
25	1.392419923377922980547579152983331921120 5
	1.392419923377932191314608189200911063469 8
27	1.392419839305767562487461598403942760914 0
	1.392419839305768243032143470927605968105 3
29	1.392419816453329288592406146120815428320 4
	1.392419816453329338874906675554826673310 8
31	1.392419810241598381890445805805973985318 4
	1.392419810241598385605600579470908459473 0
33	1.392419808553131131846714329384474489571 7
	1.392419808553131132121210896638017716887 4
35	1.392419808094173469506003158855876869186 1
	1.392419808094173469526284510377703821396 2
37	1.392419807969420009007690574166540645350 4
	1.392419807969420009009189074325282666215 6
39	1.392419807935509635330399770416650840029 7
	1.392419807935509635330510488028076467462 9
41	1.392419807926292148001835610832988215797 4
	1.392419807926292148001843791273166399823 1
43	1.392419807923786658872560704018401305740 8
	1.392419807923786658872561308435343036947 8
45	1.392419807923105619067197066761241185552 0
	1.392419807923105619067197111418955241936 1
47	1.392419807922920499438835911563942654233 7
	1.392419807922920499438835914863506473115 5
49	1.392419807922870180387681556502986145348 3
	1.392419807922870180387681556746776467444 8
51	1.392419807922856502708380429545811888474 7
	1.392419807922856502708380429563824488334 7
53	1.392419807922852784853874579237552521961 9
	1.392419807922852784853874579238883394174 5
55	1.392419807922851774270001222191378331074 8
	1.392419807922851774270001222191476663393 8
57	1.392419807922851499574000213488701971902 5
	1.392419807922851499574000213488709237247 4
59	1.392419807922851424906379880790153674356 1
	1.392419807922851424906379880790154211160 7

TABLE 8. The parameter intervals of a where the sinks of odd period persist, that is, parameter intervals of a between saddle-node bifurcation and period-doubling bifurcation.

period	parameters at saddle-node and period-doubling bifurcations
8	1.38661224375934375000000000000000000000000
	1.38666432098684375000000000000000000000000
10	1.39044286145212302999892578125000000000000
	1.39044579392295987770009765625000000000000
12	1.39187112330620198259991147812652587890 62
	1.39187133318130698151685453598785400390 63
14	1.39227050967972309570312500000000000000000
	1.39227052510069965820312500000000000000000
16	1.39237923505331439290232849121093750000000
	1.39237923619107333287294006347656250000000
18	1.39240878082091480599467724498714871633 46
	1.39240878090494237475521399194349713552 41
20	1.39241681067768535736114046863187587131 26
	1.39241681068389294914641711991551630088 39
22	1.39241899322576563366043401937323967835 23
	1.39241899322622426644848420814149394761 77
24	1.39241958647357338452588391520936440130 36
	1.39241958647360727045894011982753867840 48
26	1.39241974772878562812932646493871494332 18
	1.39241974772878813180313861210499908728 28
28	1.39241979156096082930520423609878221206 10
	1.39241979156096101429050521922751813770 45
30	1.39241980347537750491491096641253489116 57
	1.39241980347537751858266019813275945692 68
32	1.39241980671394307800554096701328717026 47
	1.39241980671394307901539116134220578744 63
34	1.39241980759424702652436626697639622347 59
	1.39241980759424702659897966396185054469 11
36	1.39241980783353045236620860192451381994 08
	1.39241980783353045237172145968561581034 72
38	1.39241980789857225807975798611196178897 95
	1.39241980789857225808016530710485995173 98
40	1.39241980791625186328638189024507983272 98
	1.39241980791625186328641198540763576438 26
42	1.39241980792105751769690343742744887605 51
	1.39241980792105751769690566102727326212 55
44	1.39241980792236378636345141684158539573 01
	1.39241980792236378636345158113364817038 52
46	1.39241980792271885513942816016535262138 69
	1.39241980792271885513942817230417487544 42
48	1.39241980792281536961528177056659959197 91
	1.39241980792281536961528177146348406098 40
50	1.39241980792284160409344369956938881080 93
	1.39241980792284160409344369963565567825 25
52	1.39241980792284873512574059191303303991026
	1.39241980792284873512574059193522656827 92
54	1.39241980792285067347653626882010940359 38
	1.39241980792285067347653626882047116011 35
56	1.39241980792285120035730902019732386924 44
	1.39241980792285120035730902019735059784 81
58	1.39241980792285134357356756031161737958 08
	1.39241980792285134357356756031161935444 03
60	1.39241980792285138250248235657743259207 98
	1.39241980792285138250248235657743273799 36

TABLE 9. The parameter intervals of a where the sinks of even period persist, that is, parameter intervals of a between saddle-node bifurcation and period-doubling bifurcation.

period	parameters at saddle-node and crisis parameter
9	1.396823348996921847450000000000000000000
	1.396848664269578097450000000000000000000
11	1.393481403358524380084492187500000000000
	1.393483122657430026712299804687500000000
13	1.392706003390789322092650465878906250000
	1.392706130415984634592650465878906250000
15	1.392497591610285067395616746063435958211 8
	1.392497601012279871979814744110310958211 8
17	1.392440954759597068258573967222160421153 6
	1.392440955454764698243296831363624654552 0
19	1.392425556467034236733077792609660870621 3
	1.392425556518409199229844547927012749651 8
21	1.392421370525885764001340005905410140655 6
	1.392421370529681925804396800438214521354 2
23	1.392420232671507861423871219916234327286 8
	1.392420232671788349083478987194266204889 2
25	1.392419923377922980546012770099701531144 2
	1.392419923377943704730420298271707968564 2
27	1.392419839305767562487389936123739508887 8
	1.392419839305769093710917101555212471959 4
29	1.392419816453329288592406666351674865470 8
	1.392419816453329401727598657365550001217 0
31	1.392419810241598381890445871262740058105 7
	1.392419810241598390249527918387543202100 3
33	1.392419808553131131846714312859830334692 2
	1.392419808553131132464329138842012991062 7
35	1.392419808094173469506003160690951841468 1
	1.392419808094173469551636114620228205614 2
37	1.392419807969420009007690574089943208527 2
	1.392419807969420009011062185568440041895 4
39	1.392419807935509635330399770421308460248 5
	1.392419807935509635330648884253380090248 5
41	1.392419807926292148001835610831861910913 9
	1.392419807926292148001854016801964704602 4
43	1.392419807923786588725607040183368607435
	1.392419807923786588725620639523532974237
45	1.392419807923105619067197066761233738558 9
	1.392419807923105619067197167241084738340 3
47	1.392419807922920499438835911563943325117 2
	1.392419807922920499438835918987939506173 2
49	1.392419807922870180387681556502986111428 4
	1.392419807922870180387681557051512129263 6
51	1.392419807922856502708380429545811885909 1
	1.392419807922856502708380429586340193555 7
53	1.392419807922852784853874579237552521841 3
	1.392419807922852784853874579240546972949 7
55	1.392419807922851774270001222191378331083 6
	1.392419807922851774270001222191599578630 3
57	1.392419807922851499574000213488701971903 6
	1.392419807922851499574000213488718318878 8
59	1.392419807922851424906379880790153674356 1
	1.392419807922851424906379880790154882165 1

TABLE 10. The parameter intervals of a where the attractor arising from the first sinks exist. In other words, the parameter intervals are the parameter intervals of periodic windows, which are between saddle-node bifurcations and crisis parameter.

period	parameters at saddle-node and crisis parameter
8	1.38661224373684375000000000000000000000000
	1.38672926028371875000000000000000000000000
10	1.39044286145275693251845703125000000000000
	1.39044945887126711464736328125000000000000
12	1.39187112330618370932073345001983642578125
	1.39187159551799077096920033005523681640625
14	1.39227050967974262695312500000000000000000
	1.39227054437685200195312500000000000000000
16	1.39237923505331432147772216796875000000000
	1.39237923761465496264733886718750000000000
18	1.39240878082091478955595106260289611681680
	1.39240878100997682724524230240907140005040
20	1.39241681067768535638090380882537768027690
	1.39241681069165240702605772352981462434220
22	1.39241899322576563373356188608340712863770
	1.39241899322679755478932280284761752567130
24	1.39241958647357338452009123896522421667400
	1.39241958647364962782993470284144033301020
26	1.39241974772878562812962649953402517517160
	1.39241974772879126139159161990490598731050
28	1.39241979156096082930517750444310339435720
	1.39241979156096124552102631003503607383250
30	1.39241980347537750491491354369046603510610
	1.39241980347537753566722964061602877709550
32	1.39241980671394307800554121432620460295330
	1.39241980671394308027648972245312309967010
34	1.39241980759424702652436625636949737776080
	1.39241980759424702669224644595909230495270
36	1.39241980783353045236620860288956957612780
	1.39241980783353045237861251201436362978350
38	1.39241980789857225807975798616307601804360
	1.39241980789857225808067445480309382894520
40	1.39241980791625186328638189025339120017840
	1.39241980791625186328644960425485004115080
42	1.39241980792105751769690343742700309287210
	1.39241980792105751769690844050879984879400
44	1.39241980792236378636345141684162335870570
	1.39241980792236378636345178649854326228300
46	1.39241980792271885513942816016535366143760
	1.39241980792271885513942818747761113752650
48	1.39241980792281536961528177056659963089470
	1.39241980792281536961528177258458839247870
50	1.39241980792284160409344369956938881806390
	1.39241980792284160409344369971848876905250
52	1.39241980792284873512574059193033040013360
	1.39241980792284873512574059194134674087020
54	1.39241980792285067347653626882010940369030
	1.39241980792285067347653626882092335532060
56	1.39241980792285120035730902019732386924440
	1.39241980792285120035730902019738400841680
58	1.39241980792285134357356756031161737958050
	1.39241980792285134357356756031162182299990
60	1.39241980792285138250248235657743259207990
	1.39241980792285138250248235657743292038550

TABLE 11. The parameter intervals of a where the attractor arising from the first sinks exist. In other words, the parameter intervals are the parameter intervals of periodic windows, which are between saddle-node bifurcations and crisis parameter.

period	length of parameter interval	ratio of period $n-1$ and n
8	5.207722750000000000e-05	
9	1.124975238281250000e-05	2.160205702734943022 84e-01
10	2.932470836847701171 88e-06	2.606698118376332942 97e-01
11	7.641183373168212890 62e-07	2.605715043148461577 4e-01
12	2.098751049989169430 58e-07	2.746630917612671141 38e-01
13	5.645531367187500000 00e-08	2.689948084703344719 93e-01
14	1.542097656250000000 00e-08	2.731536778296645473 95e-01
15	4.178676769136627197 27e-09	2.709735503585509192 53e-01
16	1.137758939970611572 27e-09	2.722773267303200412 33e-01
17	3.089639170419671903 49e-10	2.715548137551419805 75e-01
18	8.402756876053674695 63e-11	2.719656378162862081 59e-01
19	2.283339415408092773 35e-11	2.717369369468720275 24e-01
20	6.207591785276651283 64e-12	2.718646095007820577 99e-01
21	1.687185538385246748 79e-12	2.717938931466084829 48e-01
22	4.586327880501887682 54e-13	2.718330483611968763 57e-01
23	1.246616314824255091 87e-13	2.718114245874275098 47e-01
24	3.388593305620461817 43e-14	2.718232759610704584 80e-01
25	9.210767029036217579 14e-15	2.718168336624774719 88e-01
26	2.503673812147166284 14e-15	2.718203385510166299 44e-01
27	6.805446818725236632 07e-16	2.718184288107739951 38e-01
28	1.849853009831287359 26e-16	2.718194791767975161 40e-01
29	5.028250052943401124 50e-17	2.718188972972503347 26e-01
30	1.366774923172022456 58e-17	2.718192032577913479 16e-01
31	3.715154773664934474 15e-18	2.718190618425141128 03e-01
32	1.009850194328918617 18e-18	2.718191450561612165 97e-01
33	2.744965672535432273 16e-19	2.718190963323584468 48e-01
34	7.461339698545432121 52e-20	2.718190530832265062 56e-01
35	2.028135152182695221 02e-20	2.718191684233428819 97e-01
36	5.512857761101990406 37e-21	2.718190528461088468 43e-01
37	1.498500158742020865 19e-21	2.718191224368681698 04e-01
38	4.073209289816276025 0e-22	2.718191189516493213 67e-01
39	1.107176114256274332 50e-22	2.718190649537887592 66e-01
40	3.009516255593165274 88e-23	2.718191096106470615 31e-01
41	8.180440178184025701 65e-24	2.718191059104842467 42e-01
42	2.223599824386070380 16e-24	2.718190923657224110 03e-01
43	6.044169417312069931 88e-25	2.718191174071012533 04e-01
44	1.642920627746550513 32e-25	2.718190894915684241 45e-01
45	4.465771405638409614 60e-26	2.718190599240156126 81e-01
46	1.213882225405731879 79e-26	2.718191584712786962 70e-01
47	3.299563818881774136 12e-27	2.718191064853031656 96e-01
48	8.968844690049337852 06e-28	2.718191004133658289 37e-01
49	2.437903220965455156 49e-28	2.718190921145323329 64e-01
50	6.626686744314968657 32e-29	2.718191061616743375 30e-01
51	1.801259985994772183 37e-29	2.718190938390247964 23e-01
52	4.896169176684217510 82e-30	2.718191274304156843 90e-01
53	1.330872212599493535 59e-30	2.718190823424092729 26e-01
54	3.617565197250488384 23e-31	2.718191245562613267 65e-01
55	9.833231898458295800 04e-32	2.718190650974858053 36e-01
56	2.672860373148725123 05e-32	2.718191130596431668 90e-01
57	7.265344899650764160 90e-33	2.718190958509339565 91e-01
58	1.974859571196546071 47e-33	2.718191081735810017 49e-01
59	5.368046404194778428 18e-34	2.718191451426765056 25e-01
60	1.459137337050888043 32e-34	2.718190617559988502 89e-01

TABLE 12. Lengths of parameter intervals of a where the sink persists of minimum period and ratios of lengths of these of period $n-1$ and n. In other words, the parameter interval is the parameter interval between saddle-node bifurcation and period-doubling bifurcation. The ratios are about the unstable eigenvalue of the saddle fixed point.

period	length of periodic window	ratio of period $n-1$ and n
8	1.170165468750000000e-04	
9	2.531527265625000000e-05	2.163392557062242399 21e-01
10	6.597418510182128906 25e-06	2.606102094876436220 00e-01
11	1.719298905646627807 62e-06	2.606017646134085699 02e-01
12	4.722118070616484668 80e-07	2.746537007095050447 53e-01
13	1.270251953125000000 00e-07	2.690004642258268095 16e-01
14	3.469710937500000000 00e-08	2.731513955923483437 86e-01
15	9.401994804584197998 05e-09	2.709734319066513879 60e-01
16	2.561340641169616699 22e-09	2.724252346875117909 82e-01
17	6.951676299847228641 41e-10	2.714077225071007578 28e-01
18	1.890620376892912398 06e-10	2.719661122504310263 29e-01
19	5.137496249676675531 74e-11	2.717360032964286146 20e-01
20	1.396705064515391470 44e-11	2.718649312110528654 43e-01
21	3.796161803056794532 80e-12	2.717940887809361434 42e-01
22	1.031921055760916764 21e-12	2.718327377220802173 67e-01
23	2.804876596077672780 32e-13	2.718111604001932196 10e-01
24	7.624330984346387621 61e-14	2.718241150077054681 91e-01
25	2.072418440752817200 64e-14	2.718164315016919199 14e-01
26	5.633261965120370880 81e-15	2.718206832339350359 44e-01
27	1.531223527165431472 96e-15	2.718182709496472827 83e-01
28	4.162158488055919326 79e-16	2.718191311859489822 40e-01
29	1.131351919910138751 36e-16	2.718185583650313991 99e-01
30	3.075231609692556274 20e-17	2.718191886691469433 48e-01
31	8.359082047124803143 99e-18	2.718195930601954051 96e-01
32	2.270948508126918496 72e-18	2.716743890446721773 66e-01
33	6.176148259821826563 71e-19	2.719633773165522929 42e-01
34	1.678801895895949271 92e-19	2.718202065868769173 91e-01
35	4.563295392927636414 61e-20	2.718185751447629781 04e-01
36	1.240390912479405365 56e-20	2.718191144061830781 54e-01
37	3.371611478496833368 29e-21	2.718184601786022345 19e-01
38	9.164686400178109015 58e-22	2.718191718894018033 78e-01
39	2.491138320716299999 89e-22	2.718192649415572515 60e-01
40	6.771400145884097237 64e-23	2.718195167876930269 85e-01
41	1.840597010279368851 01e-23	2.718192649415572515 60e-01
42	5.003081796755921870 12e-24	2.718184246097708188 96e-01
43	1.359934016436680216 26e-24	2.718192649415572515 60e-01
44	3.696569199035773001 83e-25	2.718197467198871760 56e-01
45	1.004798509997814794 04e-25	2.718192074586105983 07e-01
46	2.731225747608889314 57e-26	2.718182521603091452 84e-01
47	7.423996181055995138 61e-27	2.718192074586105983 07e-01
48	2.017988761584050256 18e-27	2.718197467198871760 56e-01
49	5.485260178352337158 13e-28	2.718181727655708397 55e-01
50	1.490999509886463464 49e-28	2.718192868536511249 22e-01
51	4.052830764658379157 13e-29	2.718197248077562316 24e-01
52	1.101634073657876901 38e-29	2.718184246093818182 66e-01
53	2.994451108347631842 78e-30	2.718190350090412642 77e-01
54	8.139516303596188369 20e-31	2.718199766530052016 23e-01
55	2.212475467083874470 19e-31	2.718190350090412642 77e-01
56	6.013917231295872009 91e-32	2.718184820924789806 13e-01
57	1.634697524134380876 10e-32	2.718190924922553552 31e-01
58	4.443419393651083243 74e-33	2.718190569233290411 24e-01
59	1.207809036781094610 16e-33	2.718197248062731633 35e-01
60	3.283056423293797564 94e-34	2.718191637349724818 28e-01

TABLE 13. Lengths of parameter intervals of a where periodic window exists and ratio of lengths of these of period $n-1$ and n. In other words, the period window is the parameter interval between saddle-node bifurcation and crisis parameter. The ratios are about the unstable eigenvalue of the saddle fixed point.

period	ratio of parameter intervals
8	4.450415679726918962 72e-01
9	4.443859853129050771 57e-01
10	4.444876177434963312 97e-01
11	4.444360051688840047 36e-01
12	4.444512014743358754 77e-01
13	4.444418568535708190 27e-01
14	4.444455702586895972 51e-01
15	4.444457645412864739 32e-01
16	4.442044613991923449 69e-01
17	4.444452010067802496 30e-01
18	4.444444256896750654 80e-01
19	4.444459527443534435 07e-01
20	4.444454268110262585 17e-01
21	4.444451069042076593 97e-01
22	4.444456147975415126 84e-01
23	4.444460467770731585 20e-01
24	4.444446748937875968 20e-01
25	4.444453324633782292 01e-01
26	4.444476888332816523 7e-01
27	4.444502699898658737 1e-01
28	4.444455959058551293 0e-01
29	4.444461501725109534 96e-01
30	4.444617402611331906 7e-01
31	4.444453054438916793 54e-01
32	4.446821188217272565 05e-01
33	4.444462077428531129 92e-01
34	4.444443216787908413 32e-01
35	4.444452917349978960 33e-01
36	4.444451910795115784 72e-01
37	4.444462739253983302 21e-01
38	4.444618736790248814 1e-01
39	4.444586037194344261 3e-01
40	4.444519460609021593 2e-01
41	4.444493457817716407 8e-01
42	4.444460264127378477 2e-01
43	4.444457851822174816 44e-01
44	4.444447105643514268 42e-01
45	4.444446933426699066 4e-01
46	4.444459512248122817 60e-01
47	4.444457861254505045 55e-01
48	4.444472936554463157 4e-01
49	4.444462325755626598 39e-01
50	4.444459371297564797 01e-01
51	4.444490544786017645 9e-01
52	4.444605461656863425 8e-01
53	4.444613201044453576 7e-01
54	4.444473876809871170 4e-01
55	4.444478796498764019 4e-01
56	4.444458196463705280 24e-01
57	4.444458251380769796 33e-01
58	4.444459089363241628 66e-01
59	4.444496114228795946 6e-01
60	4.444479439892685785 1e-01

TABLE 14. Ratios of lengths of two parameter intervals; parameter intervals where sinks of minimum period exist and parameter intervals of periodic windows.

period	distances	rations of distances
8	1.002656899340636307 09e-02	
9	7.638042575107693758 53e-03	7.617802839765623086 85e-01
10	3.425230741800800604 59e-03	4.484435256964387941 79e-01
11	1.840590066970335173 36e-03	5.373623576678085969 73e-01
12	9.509915718584832976 00e-04	5.166775529892123706 86e-01
13	4.961293437514998793 30e-04	5.216968882089406178 27e-01
14	2.587891248281341406 57e-04	5.216162440046195700 04e-01
15	1.348348712825870995 53e-04	5.210221695835674024 74e-01
16	7.032942240073269074 29e-05	5.215966888367935273 08e-01
17	3.665675917591242330 24e-05	5.212151319407186514 89e-01
18	1.911460956863837112 64e-05	5.214484312950065757 34e-01
19	9.964721264920807768 36e-06	5.213144024280818470 79e-01
20	5.195496392894713908 21e-06	5.213890338493079634 93e-01
21	2.708666718151392451 14e-06	5.213489748266837545 98e-01
22	1.412216047621964175 10e-06	5.213694391260404513 75e-01
23	7.362729082834397782 07e-07	5.213599643788586393 47e-01
24	3.838656953609487479 39e-07	5.213633301487356116 00e-01
25	2.001335016361647058 89e-07	5.213633415405334945 05e-01
26	1.043418967428473907 25e-07	5.213614706674002773 55e-01
27	5.440014638770575534 05e-08	5.213643616406165331 61e-01
28	2.836210995447362561 00e-08	5.213609123831946934 37e-01
29	1.478700199287497394 27e-08	5.213646663316240200 70e-01
30	7.709362395701100565 50e-09	5.213607463781914324 96e-01
31	4.019389848750607530 59e-09	5.213647565707771355 74e-01
32	2.095551894630070918 29e-09	5.213606973907880688 56e-01
33	1.092546959045629831 28e-09	5.213647831128982022 82e-01
34	5.696110288053408669 95e-10	5.213606830253886295 34e-01
35	2.969751349130906370 81e-10	5.213647908748253104 01e-01
36	1.548311579355388074 15e-10	5.213606788354517689 27e-01
37	8.072351462765173589 18e-11	5.213647931333015815 15e-01
38	4.208606628606257462 08e-11	5.213606776190347745 20e-01
39	2.194219327056469120 03e-11	5.213647937876097987 59e-01
40	1.143979674427203898 30e-11	5.213606772673200137 37e-01
41	5.964307272709835811 63e-12	5.213647939764483164 58e-01
42	3.109555278526041564 21e-12	5.213606771659904320 20e-01
43	1.621212647316004505 94e-12	5.213647940307639561 34e-01
44	8.452365235875628839 11e-13	5.213606771368904579 69e-01
45	4.406765660406737641 31e-13	5.213647940463395737 24e-01
46	2.297514328656531185 47e-13	5.213606771285574040 23e-01
47	1.197843084788760447 31e-13	5.213647940507939243 65e-01
48	6.245082817763771566 43e-14	5.213606771261773013 21e-01
49	3.255966317121496490 03e-14	5.213647940520646716 98e-01
50	1.697532803792280885 03e-14	5.213606771254990819 74e-01
51	8.850338406464004480 77e-15	5.213647940524263834 33e-01
52	4.614218424382177100 34e-15	5.213606771253062309 24e-01
53	2.405691038541399240 30e-15	5.213647940525291342 58e-01
54	1.254232708808093412 95e-15	5.213606771252515005 74e-01
55	6.539127779217139066 85e-16	5.213647940525582680 54e-01
56	3.409244086781088332 70e-16	5.213606771252359957 56e-01
57	1.777459841179552321 14e-16	5.213647940525665147 17e-01
58	9.266976663602780354 34e-17	5.213606771252316106 23e-01
59	4.831475379709225139 50e-17	5.213647940525688452 57e-01
60	2.518941275479081142 29e-17	5.213606771252303722 70e-01

TABLE 15. Distances between stable manifolds and peaks of unstable manifolds. We estimate the positions of the sinks by the distances.